UNCLASSIFIED

AD NUMBER

AD480293

NEW LIMITATION CHANGE

TO

Approved for public release, distribution unlimited

FROM

Distribution authorized to U.S. Gov't. agencies and their contractors; Administrative/Operational Use; AUG 1965. Other requests shall be referred to Army Electronic Command, Fort Monmouth, NJ.

AUTHORITY

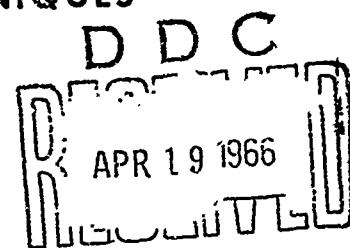USAEC ltr 24 Jul 1971

Final Report

HF COMMUNICATION EFFECTS:
PHASE-STABLE DATA REDUCTION TECHNIQUES
AND SYSTEM TEST RESULTS

By: R. A. SHEPHERD   B. C. TUPPER   J. B. LOMAX

Prepared for:

D D C

APR 19 1966

STANFORD RESEARCH INSTITUTE

MENLO PARK, CALIFORNIA

*SRI

STANFORD RESEARCH INSTITUTE

MENLO PARK, CALIFORNIA

SRI

(18) **DASA 1691**
(19)

(11) August 1965,

(9) Final Report,

(12) 69p.

HF COMMUNICATION EFFECTS: PHASE-STABLE DATA REDUCTION TECHNIQUES AND SYSTEM TEST RESULTS.

Prepared for:

U.S. ARMY ELECTRONICS COMMAND
FORT MONMOUTH, NEW JERSEY

(15)

CONTRACT DA-36-039-SC-87197

(10)

By: R. A. SHEPHERD, B. C. TUPPER, J. B. LOMAX.

(16) SRI -3670

Approved: W. R. VINCENT, MANAGER
COMMUNICATION LABORATORY

D. R. SCHEUCH, EXECUTIVE DIRECTOR
ELECTRONICS AND RADIO SCIENCES

Copy No. 1

/332500/

FOREWORD

A program of research was undertaken in 1961 with the objective of
determining the effects of high-altitude nuclear explosions on HF radio
communications, using naturally occurring distrubances to simulate
nuclear disturbances. Before the program reached the field test phase,
equipment and personnel were diverted to a nuclear field test program.
After that activity, a revised program was put into effect with the
objective of developing background information and techniques necessary
for the prediction of HF communication performance in a disturbed environ-
ment. A program of research in high latitudes was undertaken, and this
report is one of a series of final reports, having the general title
"HF Communication Effects," which were prepared at the end of the program.
Given below is a complete list of the reports, of which the first,
"Executive Summary," discusses all programs; the others discuss specific
details, as indicated by their titles.

"HF Communication Effects," Final Reports:

"Executive Summary"	DASA 1724
"Experimental Justification of the Gaussian Channel Model"	DASA 1690
"Frequency Dispersion and Doppler Shift"	DASA 1697
"Ionospheric and Mode-of-Propagation Measurements"	DASA 1701
"Prediction of Propagation Parameters Affecting Error Rate"	DASA 1723
"Propagation in the High-Latitude Ionosphere"	DASA 1700
"Physics and Chemistry of the Ionosphere"	DASA 1702
"Phase-Stable Data Reduction Techniques and System Test Results	DASA 1691
"Automatic Analysis of Oblique-Incidence Sounder Data"	DASA 1705

ABSTRACT

Data-reduction techniques are discussed for the phase-stable CW
system developed by Stanford Research Institute under contract from the
U.S. Army Electronics Command and the Defense Atomic Support Agency.

An experiment was conducted in which signals were received at a
site near Palo Alto over a transauroral path from Thule, Greenland and
over a mid-latitude path from Fort Monmouth, New Jersey.

Fixed-frequency, 7.366-Mc phase-stable data collected in analog
form on magnetic tape during the field portion of the experiment were
digitized and reduced on an IBM 7090 computer to plot form. Examples
of distributions of amplitude, rate of change of amplitude, and rate of
change of phase are presented. Power spectra of the received signal are
shown.

Several special tests were conducted to determine the resolution
of the equipment and the results of these tests are discussed. Equip-
ment limitations that must be considered in interpreting the data from
the phase-stable system are pointed out.

CONTENTS

CONTENTS (Concluded)

ILLUSTRATIONS

ILLUSTRATIONS (Continued)

ILLUSTRATIONS (Concluded)

TABLES

I BACKGROUND

The purpose of the simulation project was to provide information on propagation of HF radio signals in a nuclear environment, specifically, to determine the effects of high-altitude nuclear explosions on military HF communications.[1]* Auroral and nuclear effects on the ionosphere have the same qualitative causative mechanism: the presence of charged particles in a magnetic field, resulting in field-aligned ionization. Quantitative information on the amount of aurora-producing solar radiation is not available for a specific ionospheric region affecting a point-to-point communication path. However, widespread solar-induced geomagnetic activity was compared with simultaneous HF propagation measurements under this project.

Recent work at SRI has been concerned with characterizing a radio channel by means of a fundamental quantity called the "channel-scattering function."[2,3,4] Briefly, this scattering function is the density of power scattered by the channel as a function of Doppler shift, time delay, and angular distribution. This physical description of the path is extremely useful in computing the time-, frequency-, and angle-dispersive channel effects on a communication system.

Spreading of a signal in time is the result of variations in the propagation time, attributable both to mode geometry and to scattering from irregularities not on the optimum ray path. Frequency spreading is the result of ionospheric layer movements and of variations with time in the electron density along the ray path, giving rise to Doppler frequency shifts of the various rays. Angular spreading is the variation of the azimuth and elevation angles of arrival, and the dispersion about these angles, of the various incoming modes.

---

* References are listed at the end of the report.

The simulation experiment was concerned with measuring two of these dispersive effects--time spreading and frequency spreading. The primary instrumentation of the simulation experiment consisted of a network of four oblique-incidence, step-frequency ionospheric sounders that sounded six paths. A phase-stable HF system was operated in parallel with two of these paths.[1] The complete network is shown in Fig. 1.

The most common step-frequency sounder display, called an ionogram, shows frequency and relative time delays of ionospheric modes. This display permits identification of mode structure. The ionogram provides time-delay characteristics of a signal at discrete frequencies; it does not describe the amplitude-time behavior of a signal at a given frequency. The combination of the oblique-incidence, step-frequency ionospheric sounder with a phase-stable system provided information in both the time domain and the frequency domain for the received HF signal. The dispersion of a signal in time and in frequency greatly influences the effectiveness of communication systems using either frequency-shift keying[3] or phase-shift keying.[4] These data will help in understanding HF propagation paths through auroral regions and the relationship of the received signal to influences such as geomagnetic activity.

There are five main blocks in the data reduction system as shown (see Fig. 2). The first block, containing the transmitting and receiving equipment, was discussed in Interim Report 3.[1] Following sections of this report describe data collection, analog-to-digital (A/D) conversion, and computer reduction of the data to plot form for analysis.

Phase-stable data were recorded on seven-track analog tape as shown in Fig. 3. Two data channels, PHASE and AMPLITUDE, were also recorded in parallel on a Sanborn strip-chart recorder. The strip chart was evaluated and compared with the corresponding ionogram. The data conversion and reduction was done by computer, and analog data were converted to digital form in proper format for input to an IBM 7090 computer.

Three programs were utilized for data reduction by the IBM 7090 computer. The calibration program converted digital voltage levels to
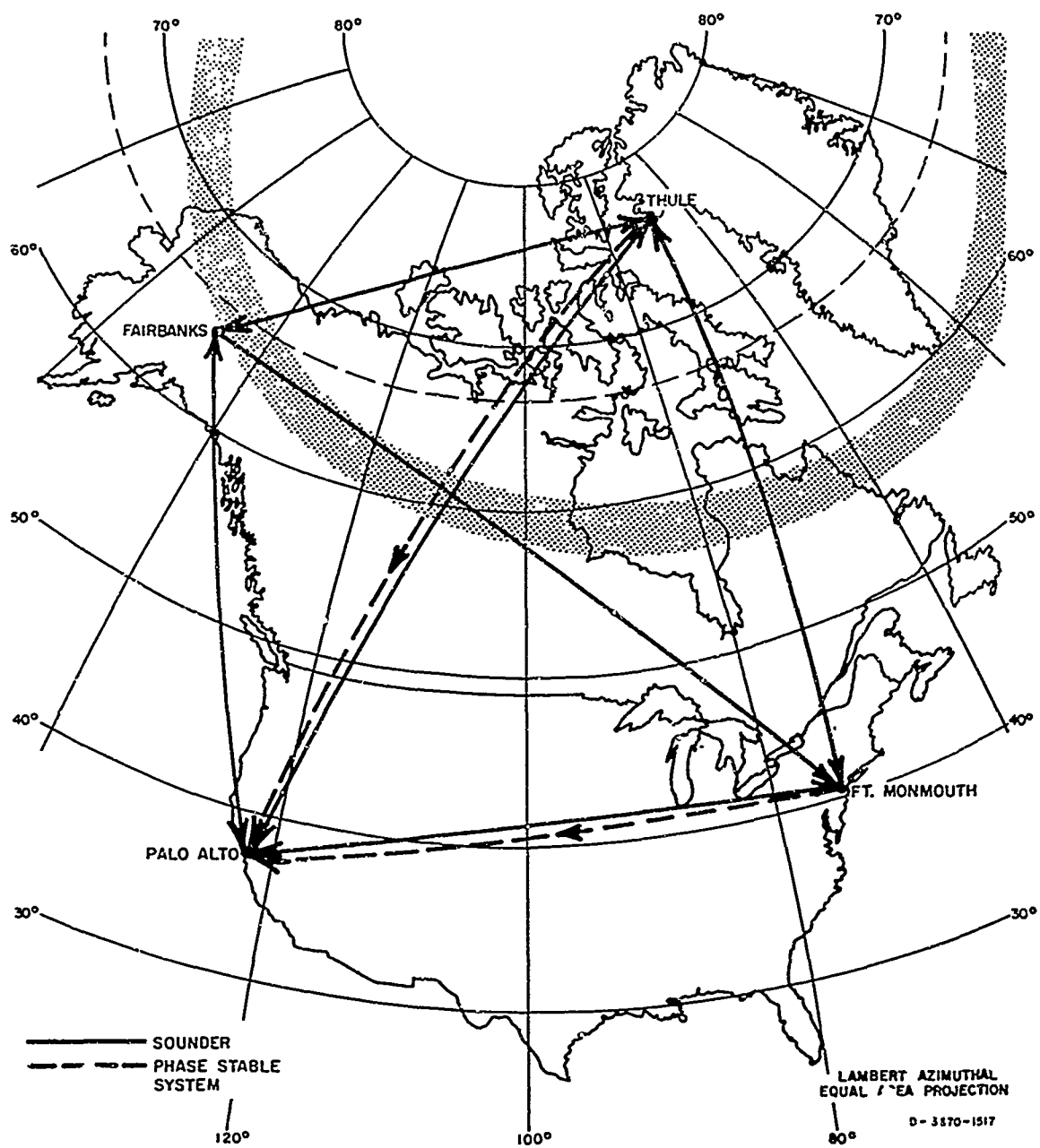
FIG. 1 LOCATIONS OF SOUNDER STATIONS AND THE PHASE-STABLE SYSTEM
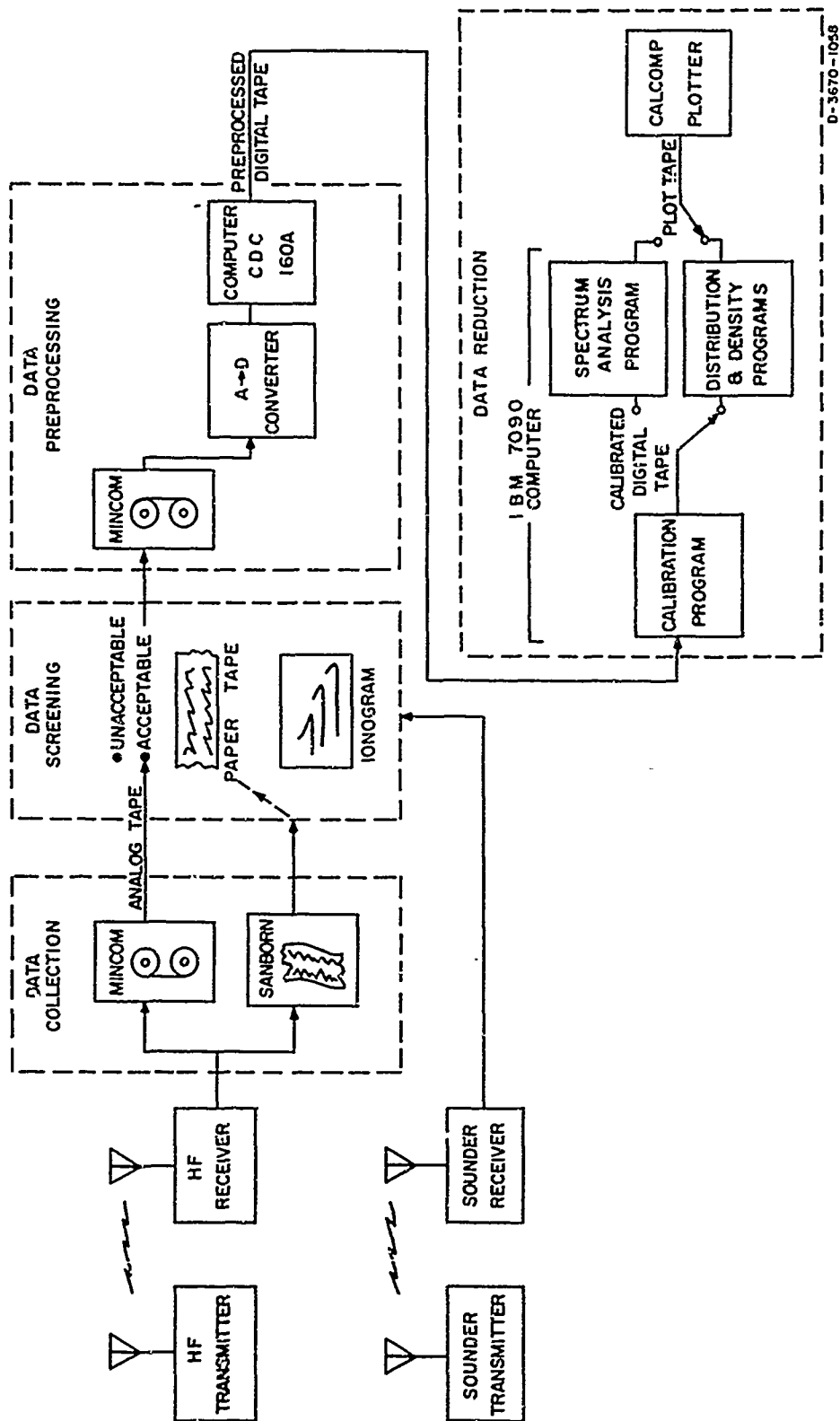
FIG. 2 BLOCK DIAGRAM — DATA COLLECTION AND REDUCTION SYSTEM

D-3670-1058

4
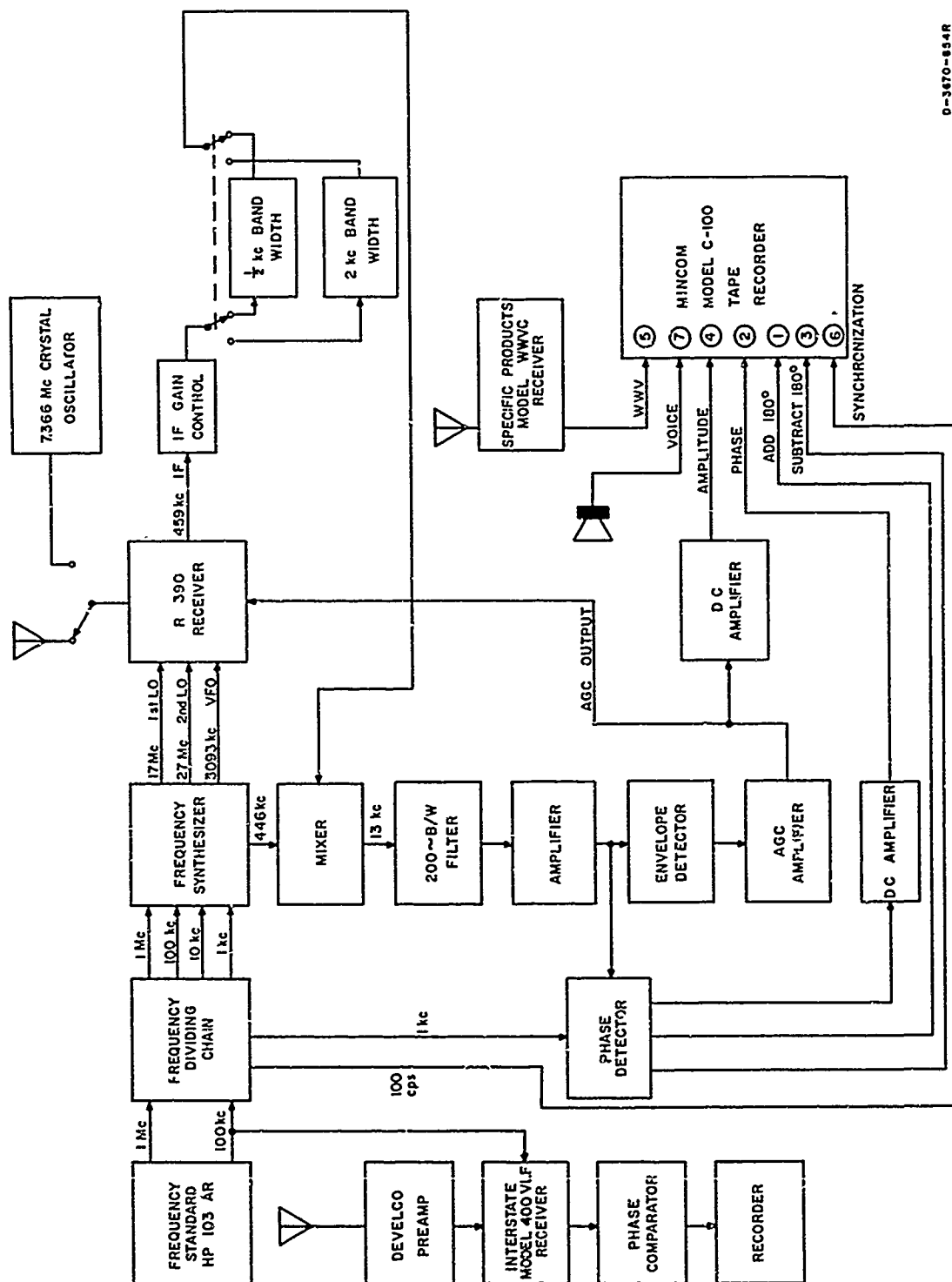
FIG. 3 BLOCK DIAGRAM — PHASE-STABLE RECEIVING SYSTEM

D-3670-854R

5

actual received signal strength, expressed both in microvolts and in decibels above 1 μv, and to phase angle in degrees. A second program derived amplitude and rate of change of amplitude densities and phase distributions. The power spectrum program compiled and plotted power density with respect to frequency.

During the data-collection phase, measurement periods of 5 minutes out of each hour were employed. The choice of a 5-minute sampling duration is a compromise between a time period which is long compared to a fading period, and a time period which is short compared to the period associated with significant ionospheric change. It implies an assumption of stationarity over the measuring interval. For most of the data obtained, this assumption appears to have been valid; however, there were several instances wherein the character of the signal was observed to change significantly during the measuring interval. Other instances were observed in which the fading period was commensurate with the measuring period. For the predominant number of measurements, however, the choice of a 5-minute data sample appears to have been a good one.

6

II DATA HANDLING TECHNIQUES

A. DATA COLLECTION

1. Recorder Track Usage

Data from the phase-stable HF system were recorded on 2500-foot,
1/2-inch, 1.5-mil instrumentation tape with a Mincom C-100, seven-track
recorder. Track utilization is shown in Table I.

Table I

TAPE RECORDER TRACK USAGE

Track Number	Recording Mode	Function
1	Direct	Add 180°
2	FM	Phase
3	Direct	Subtract 180°
4	FM	Amplitude
5	Direct	WWV
6	Direct	100-cps pulses
7	Direct	Voice

Tracks 5 and 7 were used to record the time of day, to identify the
transmitter, and to describe the calibration sequence. Track 6 contains
a 100-cps synchronization pulse train derived from the frequency standard.
The synch pulses were used to establish the 10-msec sample interval used
in the preprocessing program described in Sec. B. Tracks 1 through 3
contain phase data in pulse and in dc form. Track 4 contains amplitude
data as a dc voltage proportional to receiver input signal. Operation
of the AMPLITUDE, PHASE, and phase-associated ADD 180° and SUBTRACT 180°
channels is discussed in Interim Report 3.[1] A Sanborn 322 dc Amplifier-
Recorder was operated in parallel with the AMPLITUDE and PHASE channels
of the tape recorder. The paper chart record allowed detection of
interference and equipment malfunctions at either end of the phase-stable

HF link. Figure 4 shows typical data received at the SRI site near
Palo Alto from Thule and Fort Monmouth.

2. Calibration

Amplitude and phase calibrations were performed prior to data
transmission. A crystal oscillator provided a 7.366-Mc calibration
signal for amplitude calibration. This amplitude calibration consisted
of a sequence of 10-db steps from 10 db below 1 μv to 100 db above 1 μv.
The phase calibration consisted of two dc voltage levels generated by
signals 180° apart.[1] Following the amplitude and phase calibrations,
10 sec of background noise and interference were recorded. The calibra-
tion and noise recording are shown in Fig. 5.

3. Scheduling

Five minutes and 30 seconds of data were recorded hourly from each
of the stations between the hours of 2300Z and 1500Z. A 15-hour schedule
was maintained on a five-day-week basis from 17 December 1963 for Fort
Monmouth and 22 January 1964 for Thule to 30 September 1964. The 15-hour
data collection period commencing at 2300Z was selected as a compromise
to include periods of peak signal level and diurnal sunset and sunrise
effects on both paths. For a period of eight days commencing 18 March
1964, data were collected 24 hours a day.

Each of the phase-stable paths was sounded by a Granger Associates'
(G/A) step-frequency sounder in the 4-minute interval between Thule and
Fort Monmouth phase-stable transmissions as shown in Fig. 6. Sequential
sounder and CW operation was adopted to eliminate sounder interference on
the CW data. Generally, mode structure does not change appreciably in
the interval between the sounder sweep and the data transmission. These
paths were sounded in each direction until 15 June 1964, at which time
operation of the Deal, New Jersey receiver site was discontinued.

B. DATA PREPROCESSING

1. Channel Usage

The analog data tapes recorded at the receiver field site at Mountain
View near Palo Alto were converted to a digital tape in a form which was

8
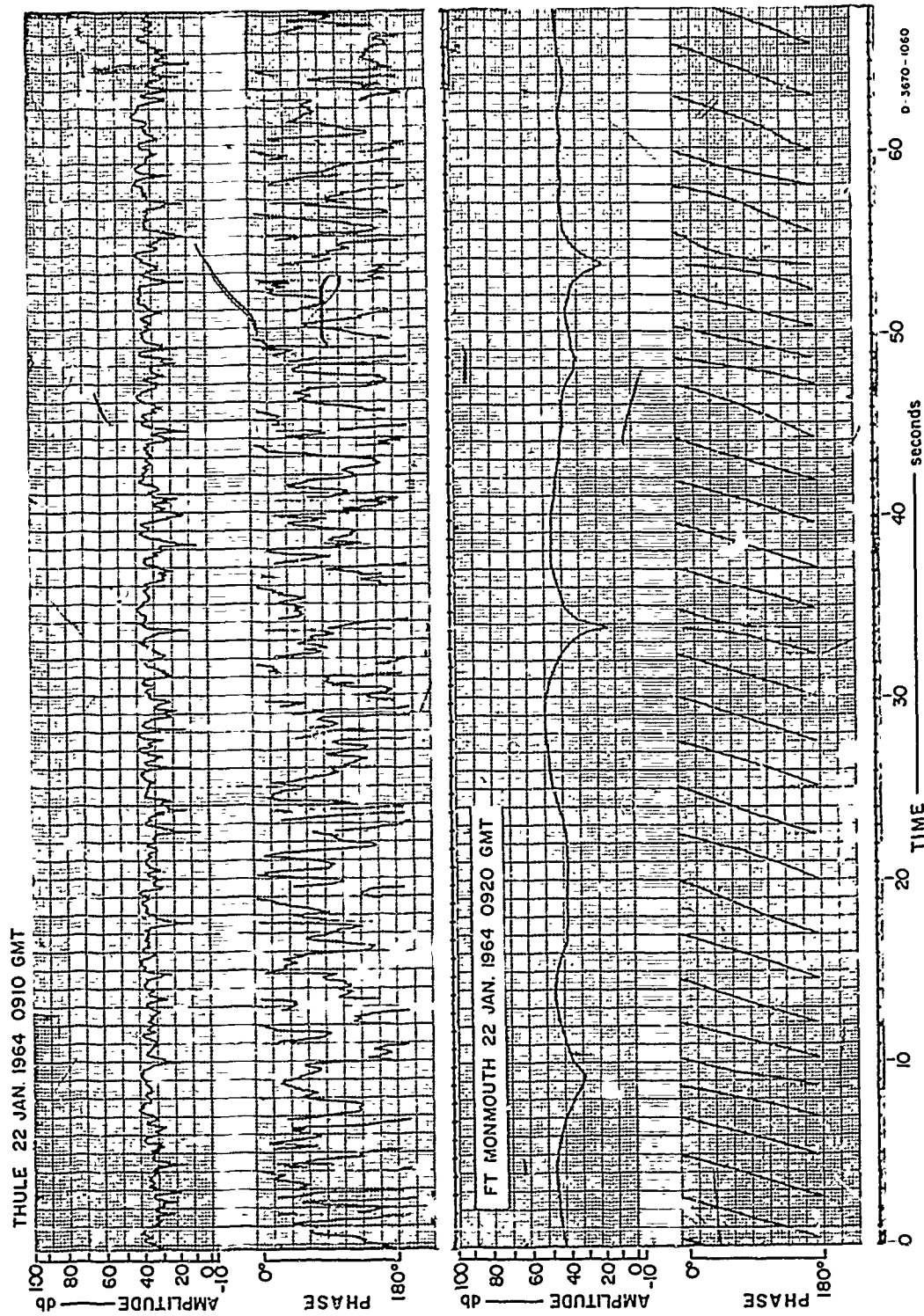
FIG. 4 SAMPLE WAVEFORMS FROM THULE AND FORT MONMOUTH — 1410 AND 1420 GMT, 22 JANUARY 1964

9
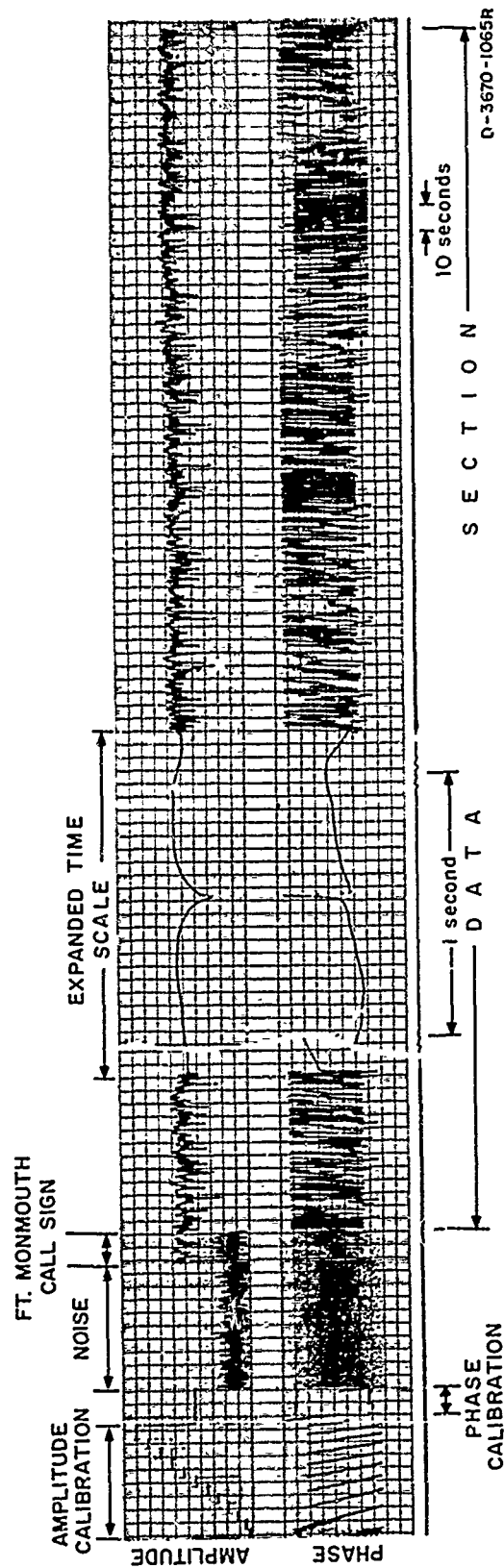
FIG. 5 SAMPLE RECORD FORMAT — PHASE STABLE HF SYSTEM

10
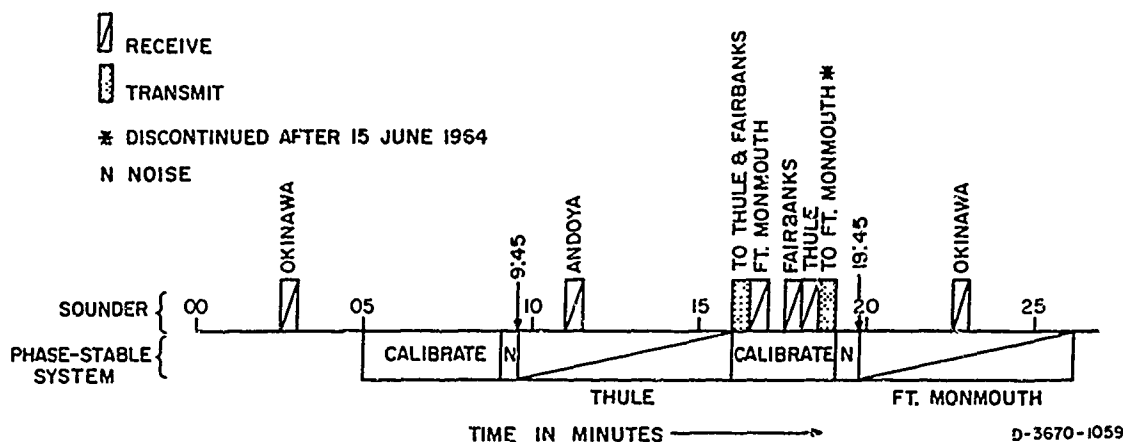
FIG. 6 SYSTEM DATA COLLECTION SCHEDULE

acceptable to a larger computer having the capacity for analysis. The
Control Data Corporation 160A computer and associated A/D conversion
equipment are shown in Figs. 7 and 8.

Data from the phase-stable HF system were recorded on seven-track
instrumentation tape in analog form as discussed in Sec. II-1. Tape
recorder channel utilization is given in Table I. Tape Channels 5 and 7
were not digitized because they were used for time of day, transmitter
identification, and calibration narrative. Tape Channel, 1 through 4
contained data which were sequentially sampled, digitized, and rerecorded
in digital form for computer analysis. Tape Channel 6, SYNCHRONIZATION,
was used to initiate the sampling process. The output waveforms for the
data and synchronization channels are shown in Fig. 9.

2. Phase and Amplitude Filtering

PHASE and AMPLITUDE were passed through identical low-pass filters
of constant time delay having a bandwidth of 50 cps to the upper 3-db
point. These filters were used to reduce noise spikes and multiples of
60-cps interference on the received carrier or generated within the
receiving system.

11
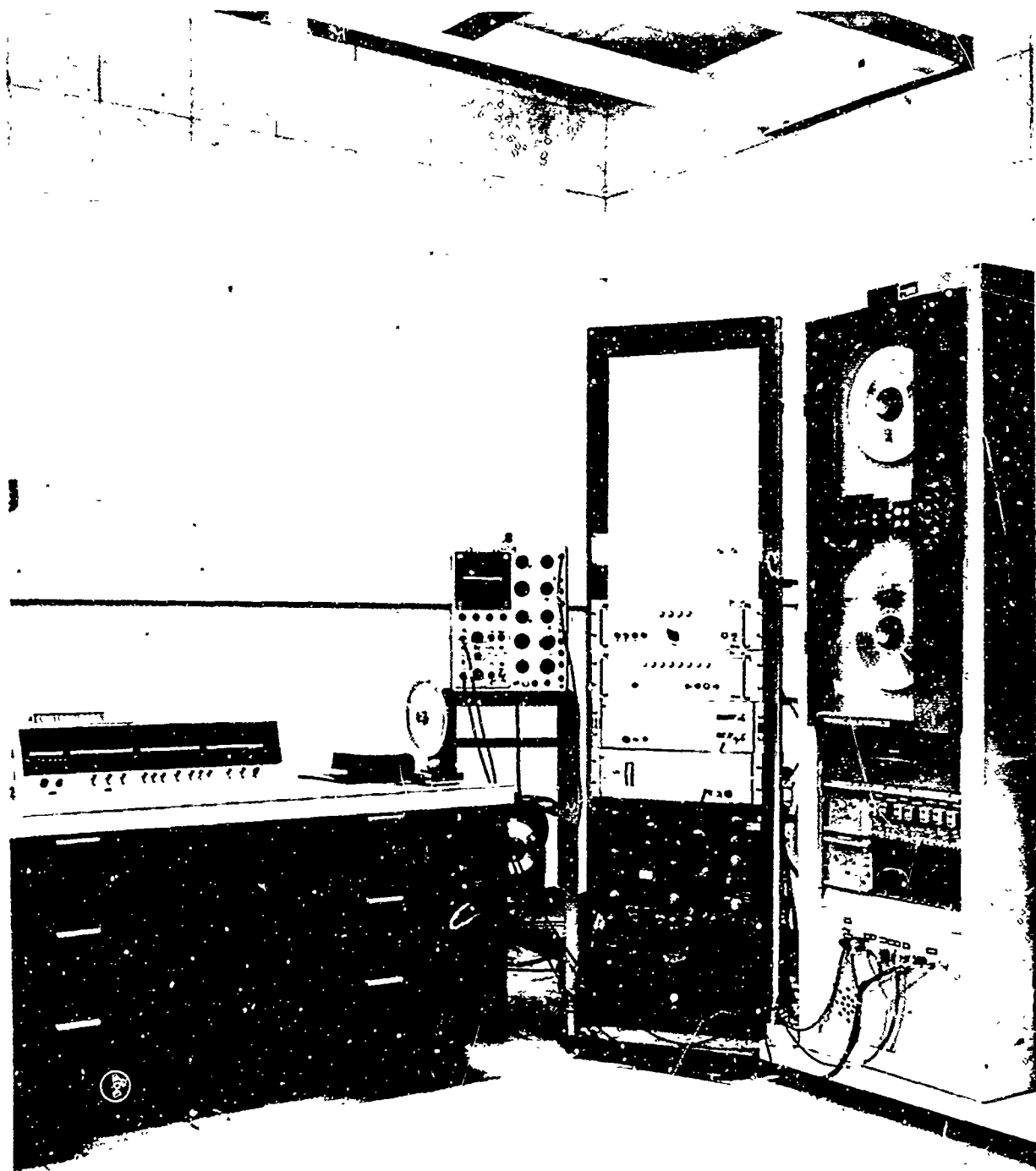
FIG. 7 PHOTOGRAPH OF ANALOG-TO-DIGITAL CONVERSION EQUIPMENT

12

FIG. 8 BLOCK DIAGRAM — ANALOG-TO-DIGITAL CONVERSION OF PHASE STABLE DATA.
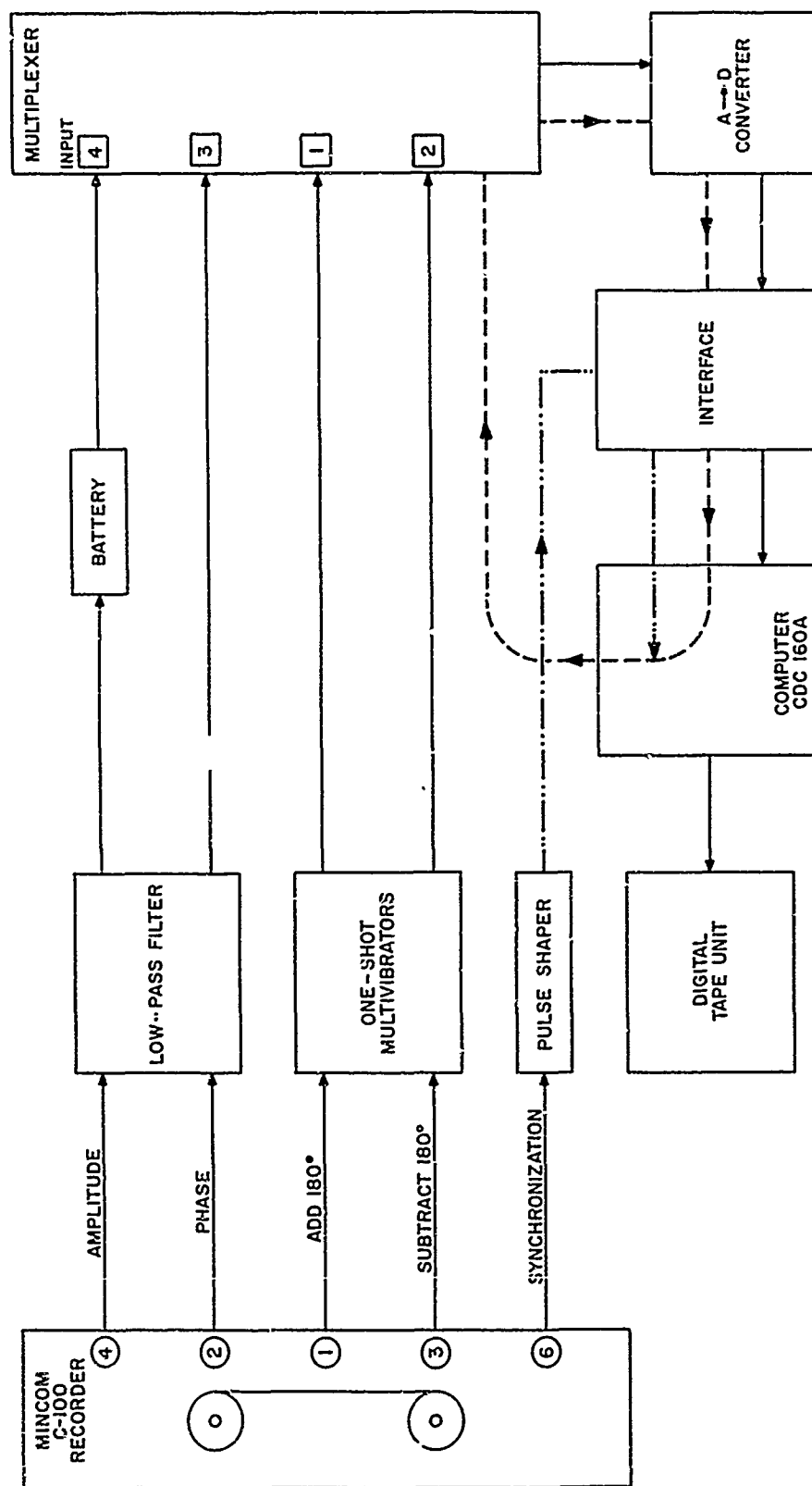
D-3670-1062

——————— DATA CHANNEL
— — — — SAMPLE CONTROL CHANNEL
—··—··— SAMPLE INITIATE CHANNEL

13
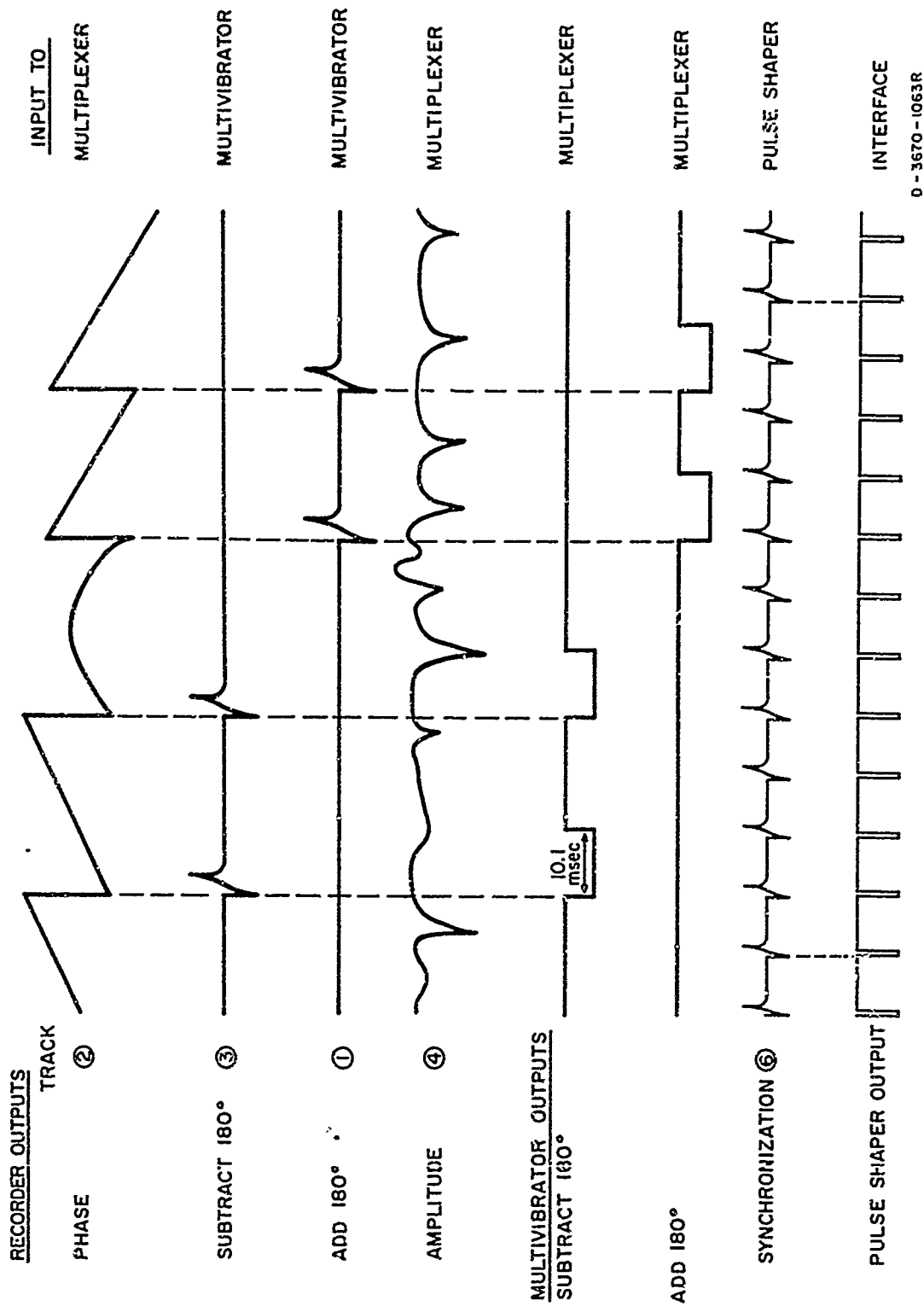
FIG. 9 TYPICAL DATA AND SAMPLE CONTROL WAVEFORMS

14

3. ADD 180° and SUBTRACT 180° Pulse Restoration

The Phase Detector, described in Interim Report 3, utilizes two auxiliary channels to indicate when the phase of the received signal increased or decreased through a predetermined 180-degree point.[1] Figure 9 shows the time relationship between the phase channel and the ADD 180° and SUBTRACT 180° auxiliary channels during playback. As the voltage for decreasing phase reaches the predetermined switching point, the PHASE channel is switched 180 degrees. The SUBTRACT 180° channel records this change in pulse form. The same procedure is used for voltage of increasing phase, the switching pulse being recorded on the ADD 180° channel. Multivibrators are used to restore the ADD 180° and SUBTRACT 180° pulses to lengths great enough to ensure that they are sampled during the digitizing process.

4. A/D Conversion Equipment

The A/D sampling and conversion process is shown in detail in Fig. 10. The equipment consists of the Control Data Corporation 160A computer and associated digital tape unit; General Radio Pulse Shaper unit; Adcom Corporation Multiplexer Model 410C-10 and A/D Converter Model 208C; and an SRI-built Interface Unit. Detailed descriptions of each unit can be found in the manufacturers' equipment manuals.

The Pulse Shaper is driven by the 100-cps SYNC PULSE which is recorded on analog tape. The SYNC PULSE triggers the Pulse Shaper which initiates the sampling sequence. The Interface Unit transforms control and data logic inputs from the A/D Converter to the proper level and polarity required by the Control Data 160A computer.

The Adcom 410C-10 Multiplexer is a high-speed electronic switch that passes signals to the Adcom Model 208C A/D Converter as analog voltages. The 208C converts the analog voltage to an eight-bit digital word, the highest bit reserved for sign. The output of the Converter passes through the interface unit into the computer. The voltage limits of the Converter are -1.28 to +1.28 dc, having a voltage range of 2.56 dc with an accuracy of ±5 mv.

15
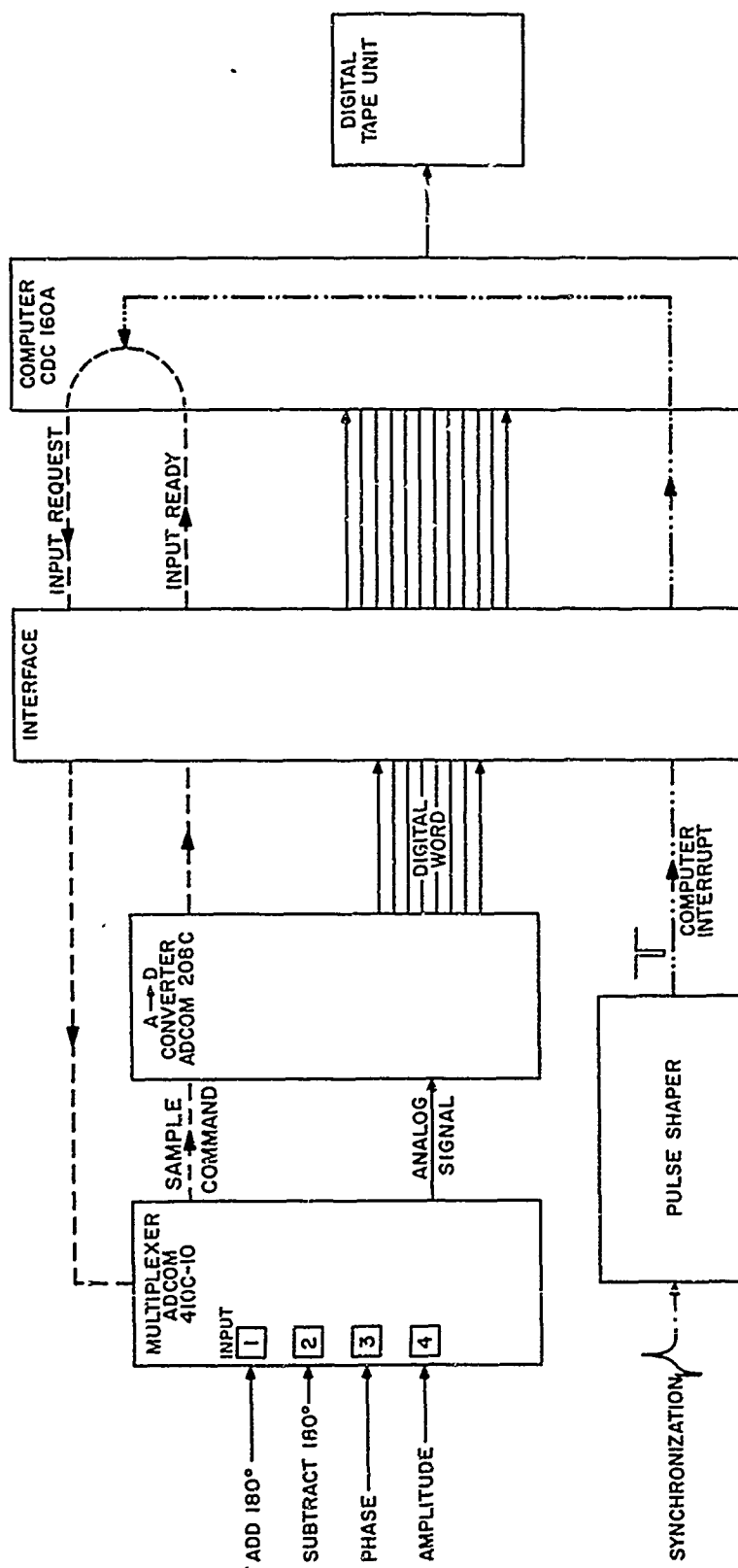
FIG. 10 BLOCK DIAGRAM — DATA SAMPLING CONTROL AND ANALOG-TO-DIGITAL CONVERSION

D-3670-1061

16

5. Sampling Control and Synchronization

The process by which the four data channels were sampled and
digitized is governed by the control loop (indicated by a dotted line
in Figs. 8 and 10). A COMPUTER INTERRUPT pulse derived from the SYNCH
PULSE initiates the sampling portion of the program in the 160A computer.
The computer sends an INPUT REQUEST through the control loop, advancing
the electronic switch in the Multiplexer to the first channel to be
digitized. The Multiplexer sends a SAMPLE COMMAND to the A/D Converter.
The Converter digitizes the analog signal of the first data channel;
the computer takes the data into temporary storage, then sends a second
INPUT REQUEST to the Multiplexer. The conversion process is repeated for
the remaining three data channels. The computer then waits for the next
INTERRUPT PULSE, 1 msec later and again samples. The total time required
to sample four data channels is approximately 100 μsec, 1 percent of the
10-msec sample interval.

6. Output Tape--Heading and Calibration

The Control Data Corporation 160A computer was programmed to pro-
duce,from the analog data, a digital tape suitable in format for input
and analysis by the larger IBM 7090 computer. Each 5-minute data record
with its calibration was converted to this format and identified by a
file number. Files consist of a heading block, AMPLITUDE and PHASE
calibration, noise level, and the 5-minute data block. Heading block
information, compiled from field site receiver logs, contains month,
day, year, and the start time of the analog record. Also contained is
the frequency of the transmitted carrier and the transmitter and receiver
identification codes. Each of the calibration levels was sampled
100 times (1 sec). Background noise was sampled 1000 times (10 sec).

7. Output Tape--Data

Following the heading and calibration, the computer accepted the
actual data. There were 30,000 samples each of AMPLITUDE, PHASE, ADD
180°, and SUBTRACT 180° taken in a 5-minute period. Two data subroutines,
limit testing and the ADD 180° and SUBTRACT 180° simplification, are of
interest.

17

A limit test was performed on each AMPLITUDE and PHASE sample. Analog tape dropouts occasionally occurred on the two FM channels. These dropouts caused the output signal to exceed the voltage range of the A/D Converter. The limit test subroutine checked for values exceeding the A/D Converter voltage limits of ± 1.28 volts. The number and types of out-of-range excursions were noted and stored in counters which were examined at the end of each 5-minute data block. These counters indicated both total and maximum successive number of samples falling outside the A/D Converter limits. The relatively low number of dropouts observed on any given record has not precluded use of the data.

The ADD 180° and SUBTRACT 180° data channels were sampled to determine the absence or presence of the pulses, and a cumulative count of 180° shifts was generated. The integer count indicated the number and direction of 180° shifts relative to zero initial phase at the beginning of the data record. This coarse phase-drift counter, when combined with the PHASE channel, yielded total cumulative phase shift and was recorded on the digital tape with each AMPLITUDE-PHASE sample.

C.   DATA PROCESSING

The processing of the data by the IBM 7090 was accomplished by three programs: the calibration program, the density and distribution plotting program, and the spectrum analysis program. The first of these programs generated the input format required by the two successive computational programs.

1.   The Calibrating Program

a.   Input

Data on the analog tape were reduced to 30,000 sets of digital numbers by the CDC 160A for input to the calibration program. Two of the three numbers of each set were digital voltages representing amplitude and phase. The third number was a cumulative count of the ADD 180° and SUBTRACT 180° pulses. The calibration program converted the amplitude voltage to an amplitude value, expressed both in decibels above

18

1 μv and in microvolts. Phase voltage was converted to degrees and combined with the 180° counter to provide the phase angle in degrees.

b. Amplitude Calibration

The 100 samples of each amplitude calibration step were converted to microvolts, averaged, and stored in the computer. This information was then used to calibrate the subsequent amplitude readings. Linear interpolation (in decibels) was employed between adjacent calibration levels.

c. Phase Calibration

Two calibration phase angles, 0° and 180°, were each sampled 100 times during digitizing. The 100 samples for each angle were averaged to ensure that the calibration was representative. Phase calibration was applied to the data by interpolation. Combination of the interpolated angle from the PHASE channel with the 180° counter yielded the actual phase reading. The 180° counter was set at zero at the beginning of the 5-minute run. The final combined count might be either positive or negative.

Because of the time required for the phase voltage to change by the amount corresponding to 180°, the two phase observations immediately following a change in either 180° counter were erroneous; therefore, these phase angles were computed as extrapolations of the phase slope during the 100-msec period immediately preceding the counter change. This extrapolation eliminated sampling erroneous values of the phase-switching transient.

d. Noise Calibration

The noise recording was calibrated after averaging 1000 observations (10 sec), and was recorded on the calibrated tape in both decibels and microvolts. Signal-to-noise ratio was computed for each 5-minute record. This ratio was computed by averaging the 30,000 amplitude readings (in microvolts) and dividing by the average noise.

19

e. Output

Data were recorded on the calibrated tape as amplitude in decibels, amplitude in microvolts, and phase in degrees, as derived from the calibration. The calibrated output tape, consisting of a heading block, noise, and scaled data, was retained for analysis by the Distribution and Density Compilation Program, and the Power Spectrum Program.

2. The Data Reduction Programs

a. Objectives

It was the objective of the data reduction scheme to present the statistics of the received signal. The data from the two phase-stable links were plotted in several forms to give a comprehensive picture of the amplitude and phase variations of the CW signal. Each data point sampled yielded amplitude and phase at a specific time. These three parameters are descriptive of the characteristics of the received CW signal at the receiver input terminals. Typical plots of data for the Fort Monmouth to Palo Alto path will be discussed in detail; plots from the Thule to Palo Alto transauroral path for the same time will be presented for comparison.

b. Amplitude Plots

Four plots display amplitude information of the signal. Figures 11(a) and 11(b) show the amplitude densities of the Fort Monmouth and Thule signal, respectively. The amplitude density plot presents frequency of occurrence of amplitude in 1-db increments. Each of the 30,000 amplitude samples in a 5-minute record was rounded to the nearest whole decibel. The computer counted amplitude samples occurring within each 1-db increment and divided by the total number of samples. The count is expressed as a percentage indicating the occurrence of signal at each decibel level. In addition, the minimum and maximum signal strengths and average noise are recorded in the upper left corner. A set of plots covering the day would show diurnal signal level fluctuations. Figure 11(a) shows that the most commonly occurring signal
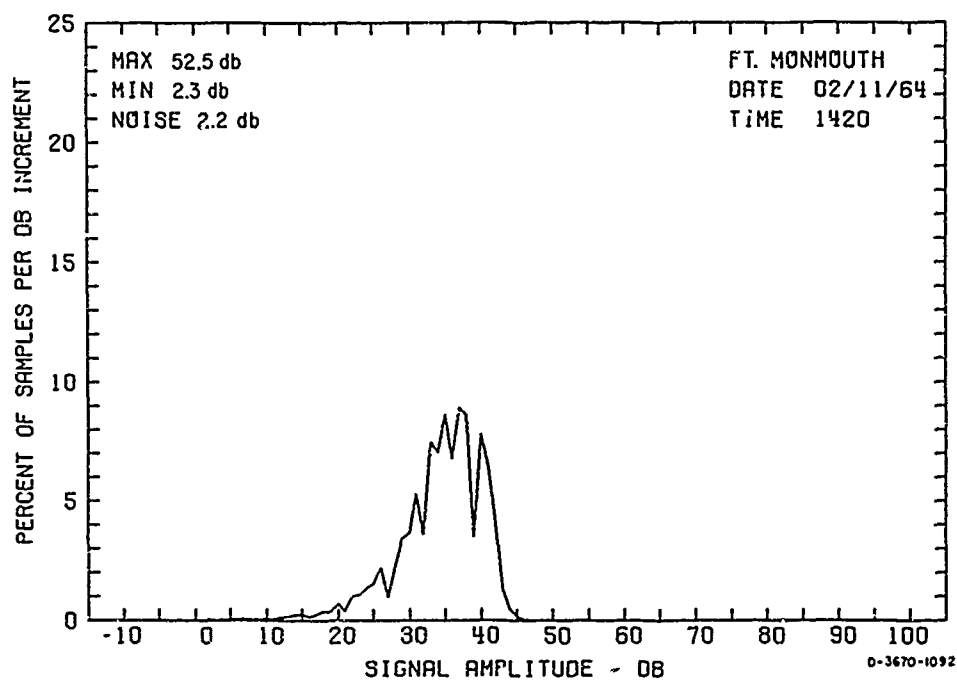
20

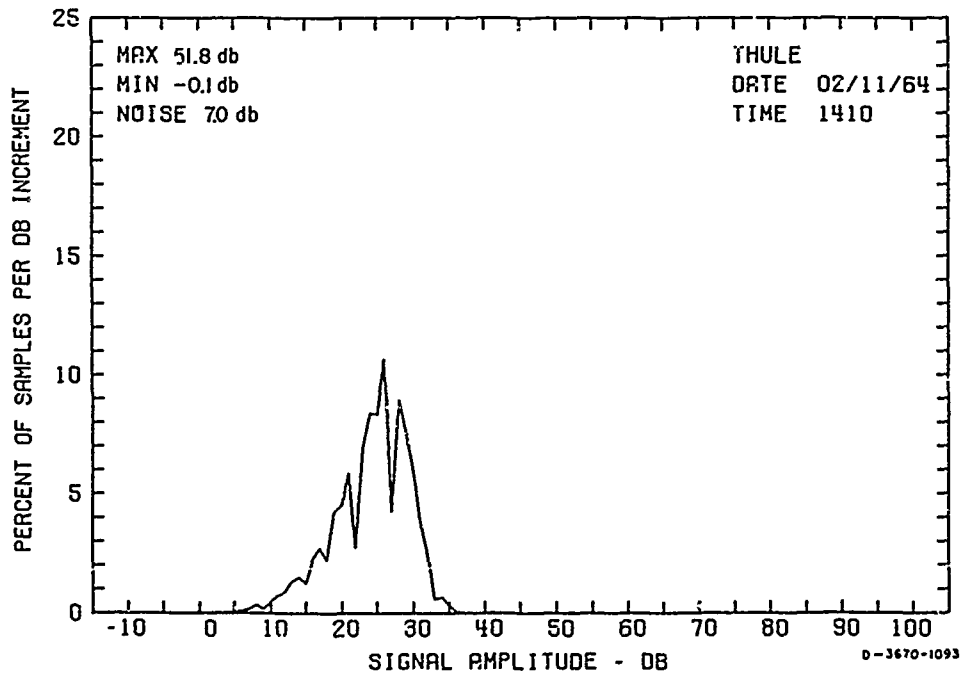FIG. 11(a) AMPLITUDE DENSITY (db) — FORT MONMOUTH, 1420 GMT,
11 FEBRUARY 1964

FIG. 11(b) AMPLITUDE DENSITY (db) — THULE, 1410 GMT, 11 FEBRUARY 1964

21

strength during the 5-minute period beginning at 1420Z is 36 db above
1 µv; levels up to more than 40 db are present. Figure 11(b) is included
for comparison.

Data for the amplitude distribution plots of Figs. 12(a) and
12(b) were compiled by the computer in a printout form and plotted by
hand. The computer successively accumulated the number of occurrences
of amplitude in each decibel increment as a percentage of total sample
size. This value was subtracted from 100 percent, giving a percentage
of the remaining 30,000 samples not yet counted. A plot of these per-
centages is an approximation to 1 minus the integral of the amplitude
density. A Rayleigh distribution plotted on this special graph paper
will be a straight line with a slope of minus 45°. This type of plot
has been used by others in the study of fading.[5,6] To show the close
approximation of the experimentally obtained distribution to a Rayleigh
distribution, a Rayleigh distribution with the same median value (the
level which is exceeded 50 percent of the time or 34.5 db in this example)
has been drawn on Fig. 12(a) for comparison.

Figures 13(a) and 13(b) are amplitude-density plots with a
linear abscissa. The ordinate is scaled in percent of samples per
microvolt interval rather than in percent of samples per decibel inter-
val. Table II gives the class intervals for the abscissa.

Table II

CLASS INTERVALS FOR AMPLITUDE DENSITY IN MICROVOLTS

Between 0 and 10 µv,	10 intervals of 1-µv width
Between 10 and 100 µv,	9 intervals of 10-µv width
Between 100 and 1000 µv,	18 intervals of 50-µv width
Between 1000 and 10,000 µv,	72 intervals of 125-µv width

If the frequency of occurrence of signal within each of these class intervals were plotted directly, the result would be misleading, since the class interval is not constant throughout the range of signal levels. To correct this, the frequency of occurrence of signal within each class interval was normalized by division by the width of the class interval. That figure, divided by the total number of samples, is occurrence expressed in percent per microvolt interval. The density plot of Fig. 13(a) was drawn by connecting the percentages at the mean of each class interval. The computer selected an appropriate abscissa scale proportional to the range of amplitude data.

Figures 14(a) and 14(b), the amplitude change density plots, show how the amplitude changes with time. Decreasing and increasing amplitude change is shown on the abscissa. Amplitude changes for time intervals of 10, 20, 40, 80, and 160 msec are represented by separate curves. The plot shows the percentage of occurrence of amplitude changes within 0.5 db increments.

The amplitude change density plots were developed from the calibrated magnetic tape by the IBM 7090 computer. Each of the 30,000 amplitude samples was compared with the previous 10-msec, 20-msec, 40-msec, 80-msec, and 160-msec sample point to determine the amount and direction of amplitude change. Amplitude differences for Figs. 14(a) and 14(b) were rounded to the nearest one-half decibel, and in later plots, to the nearest whole decibel. The number of amplitude change samples falling into each increment (for a given time interval) was normalized by division by the total number of samples for that time interval. For example, since 29,999 amplitude comparisons were possible for the 10-msec interval, the 10-msec curve was normalized by division by 29,999; the 160-msec curve was normalized by division by 29,984.

23

FIG. 12(a)   AMPLITUDE DISTRIBUTION— FORT MONMOUTH, 1420 GMT, 11 FEBRUARY 1964

24

FIG. 12(b) AMPLITUDE DISTRIBUTION — THULE, 1410 GMT, 11 FEBRUARY 1964

25
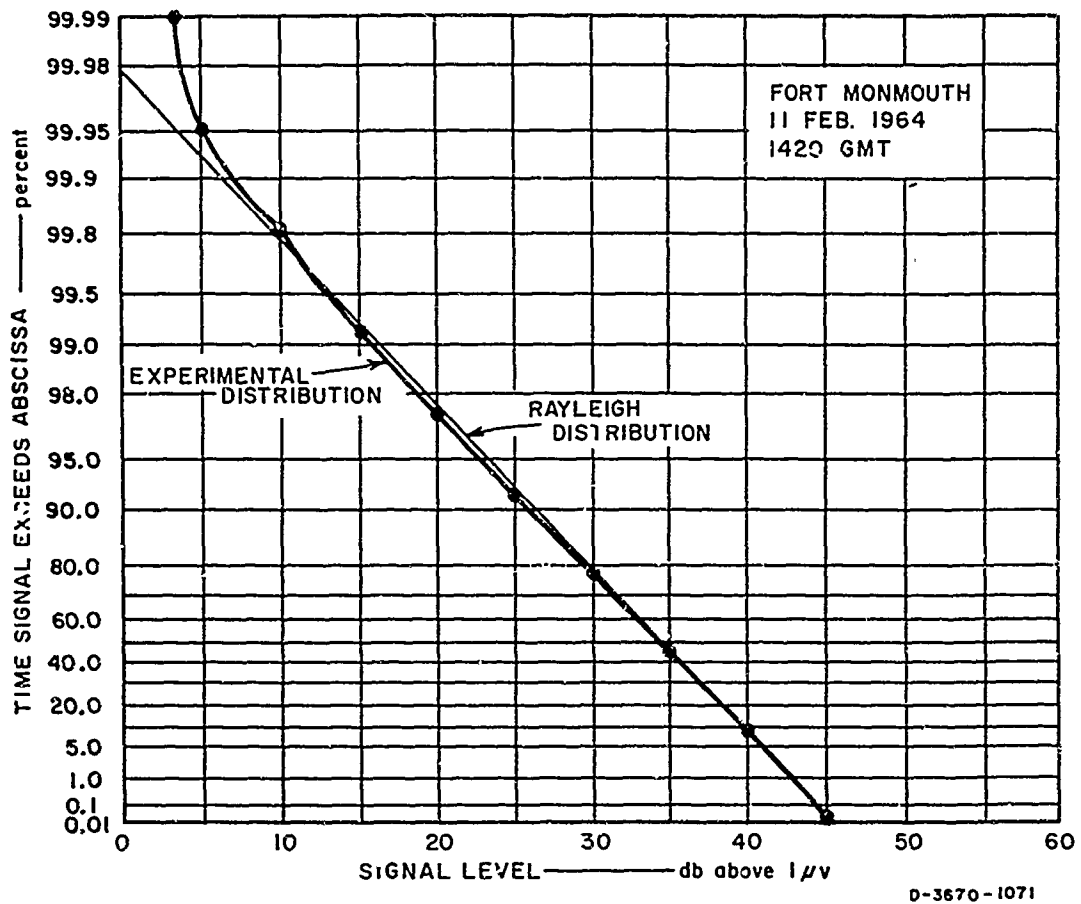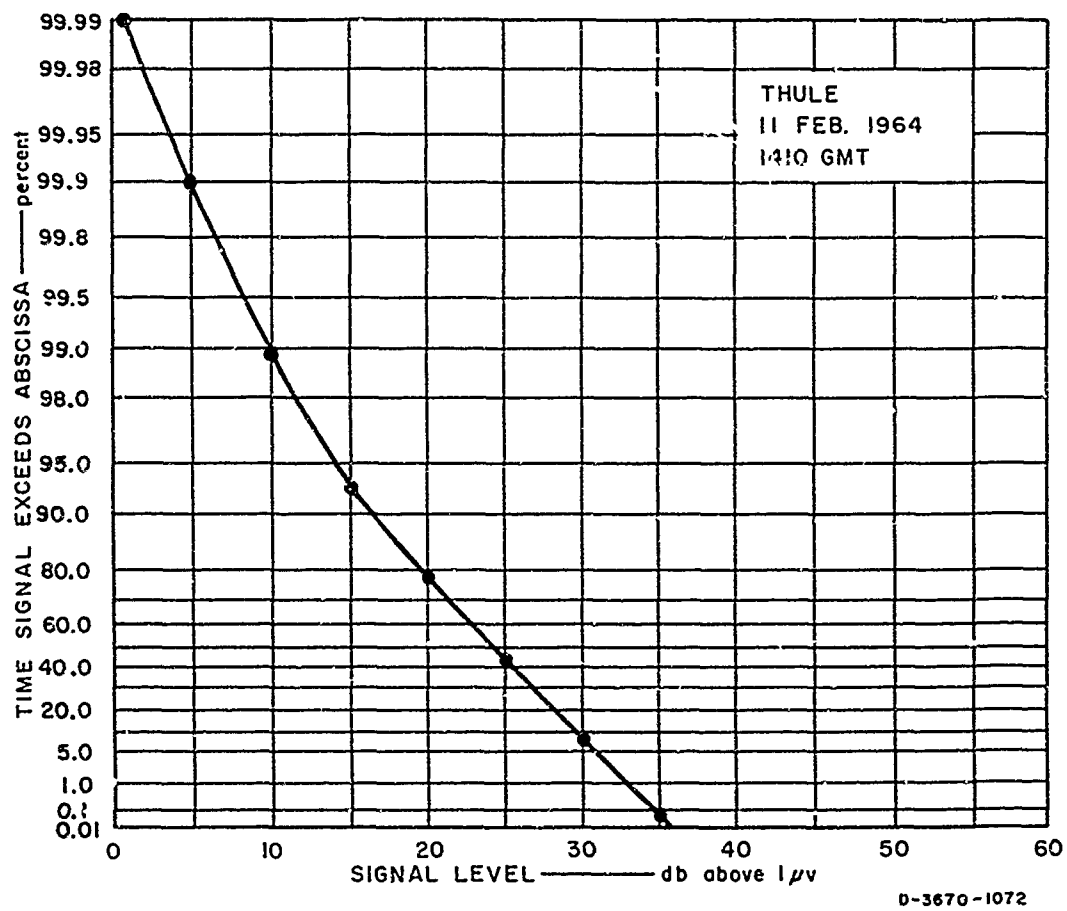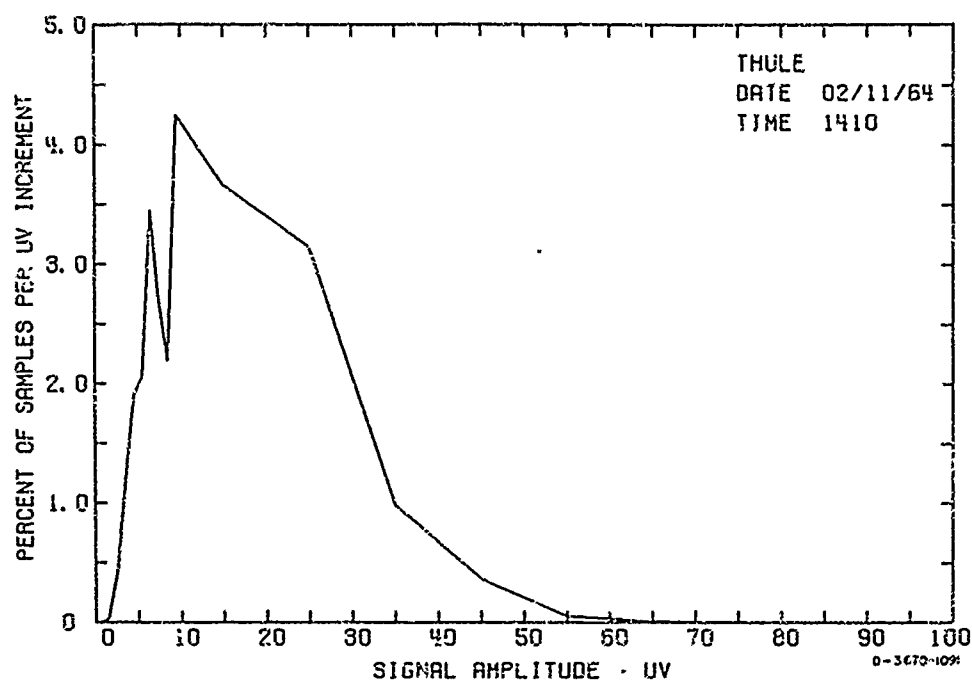
FIG. 13(a) AMPLITUDE DENSITY (μv) — FORT MONMOUTH 1420 GMT
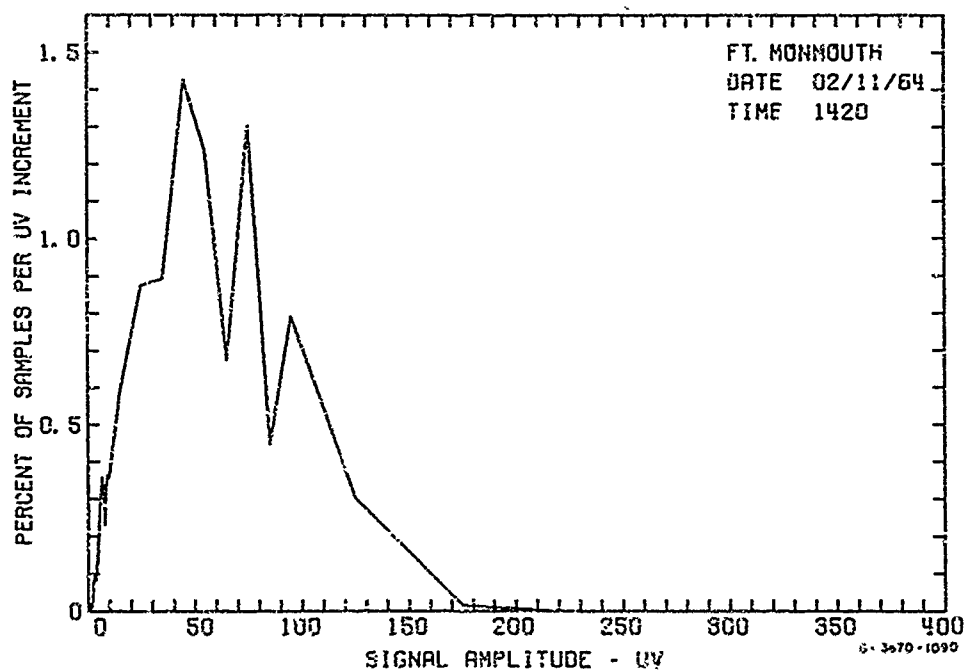11 FEBRUARY 1964

FIG. 13(b) AMPLITUDE DENSITY (μv) — THULE 1410 GMT, 11 FEBRUARY 1964
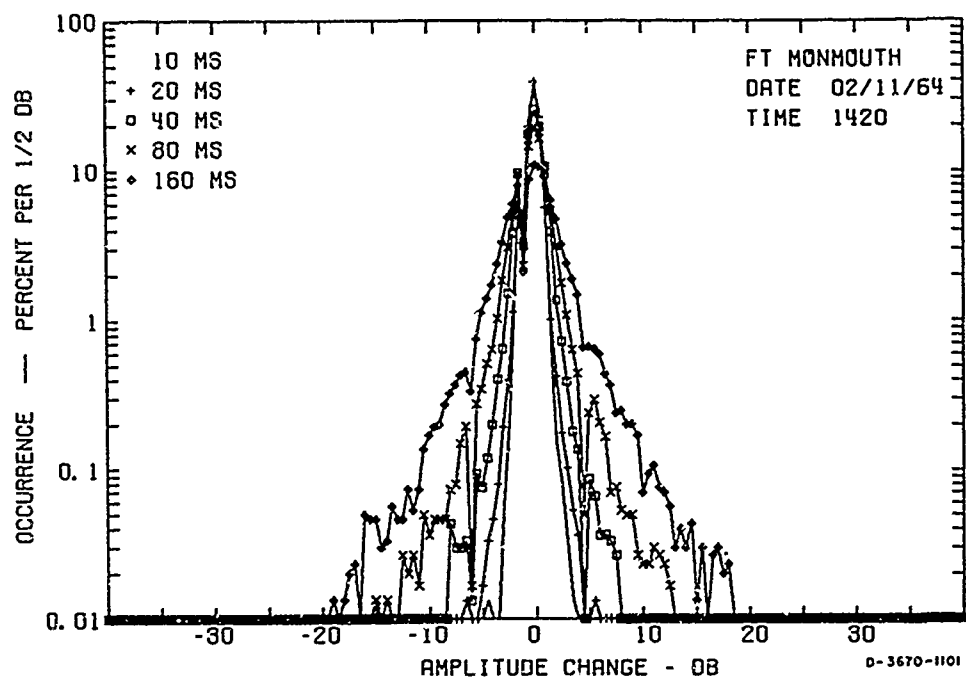
26

FIG. 14(a) AMPLITUDE CHANGE DENSITY — FORT MONMOUTH 1420 GMT, 11 FEBRUARY 1964
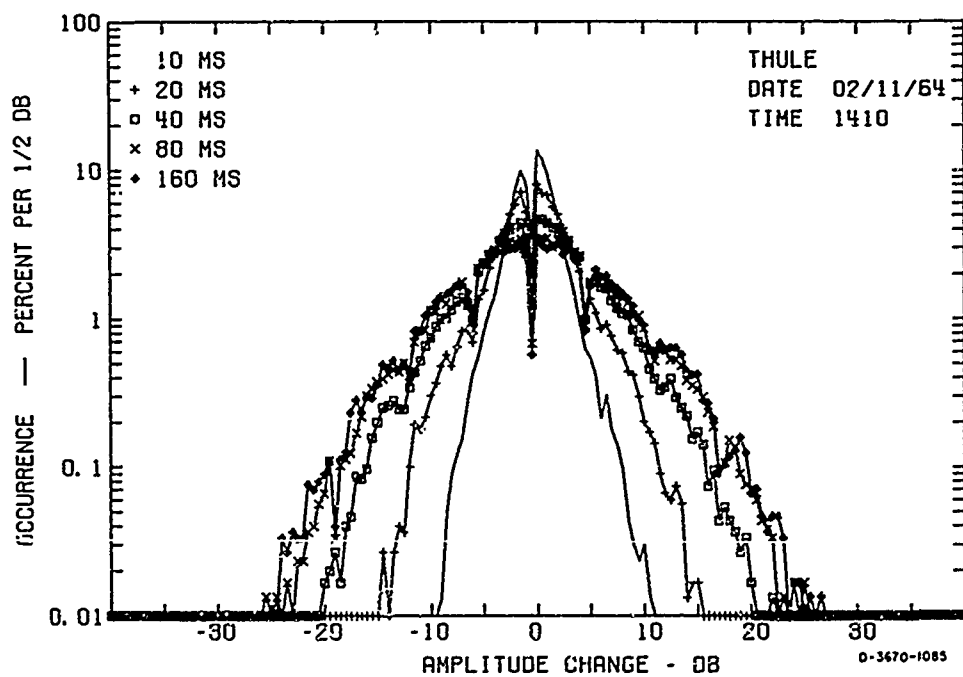

FIG. 14(b) AMPLITUDE CHANGE DENSITY — THULE 1410 GMT, 11 FEBRUARY 1964

27

c. <u>Phase Plots</u>

The phase of the received signal varies with time. Diurnal changes in phase (or frequency), as the reflecting ionospheric layers rise in the evening and drop again with sunrise, are slow compared to phase shifts caused by the interference between two or more modes. The daily variations in frequency, which usually amount to less than one cycle per second, will not affect the operation of phase-shift communication systems as greatly as the more rapid phase shifts induced by mode interference. The time intervals for the phase-shift plots were chosen to display the latter. Figures 15(a) through 15(e) show magnitude, direction, and frequency of occurrence of phase shifts. The form of these plots is similar to that used by General Dynamics[7] and by Koch, Beery and Petrie.[5] In the computer, the amplitude corresponding to each phase sample was compared with the average received noise level and the signal-to-noise ratio was computed for each sample in the record. Separate phase distributions were plotted for five ranges of signal-to-noise ratio (S/N). The phase data for points for which the S/N was greater than 40 db was grouped and plotted. Similarly, those points for which the S/N were between 30 and 40 db, 20 and 30 db, 10 and 20 db, and less than 10 db were also grouped and plotted separately. This procedure shows behavior of phase change for various signal-to-noise-ratio ranges.

Phase change was computed and plotted as a family of curves for time intervals between 10 and 160 msec. The resolution on these plots is to the nearest whole degree. The phase change curve is discontinuous at zero degrees on this plot. Phase changes of exactly zero degrees were divided equally between the positive and negative values and plotted so that the total percentage of positive and negative phase changes would add to 100 percent. A computer printout provided cumulative phase drift over the entire 5-minute period and the number of samples falling into each signal-to-noise ratio interval. From the latter, it is possible to determine the percentage of time a given rate of phase change occurred within each signal-to-noise ratio group. For example, Fig. 15(c) indicates 0.47 percent of the time the phase shift was $\geq +45°/40$ msec when the S/N was between 20 and 30 db. In that range are 7399 samples.

28

FIG. 15(a) PHASE DISTRIBUTION (S/N > 40 db) — FORT MONMOUTH
1420 GMT, 11 FEBRUARY 1964

FIG. 15(b) PHASE DISTRIBUTION (S/N 30-40 db) — FORT MONMOUTH
1420 GMT, 11 FEBRUARY 1964

FIG. 15(c) PHASE DISTRIBUTION (S/N 20–30 db) — FORT MONMOUTH
1420 GMT, 11 FEBRUARY 1964

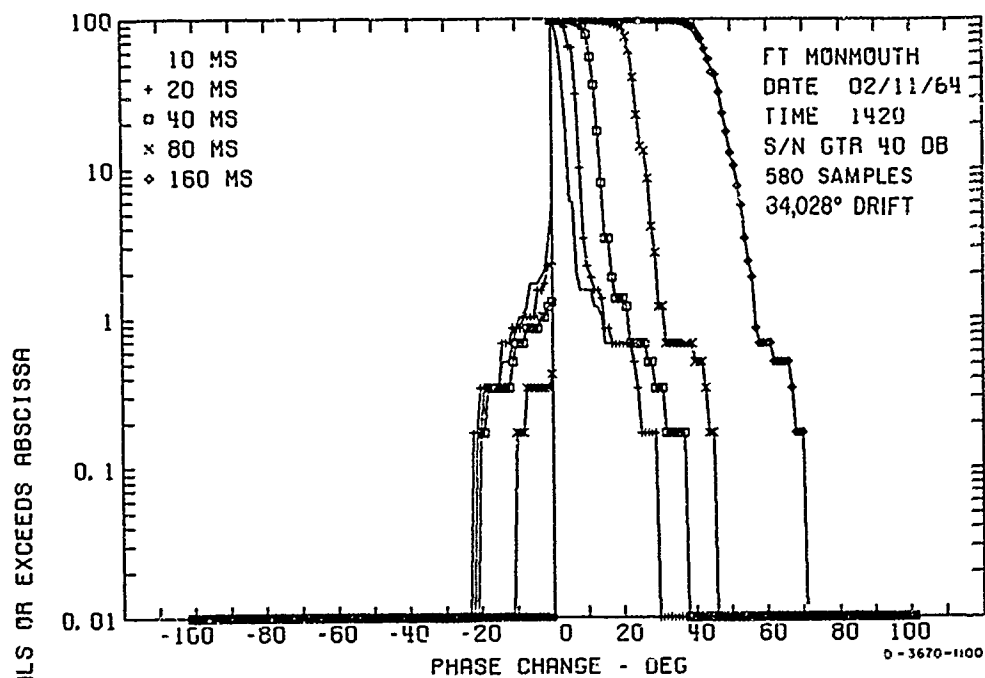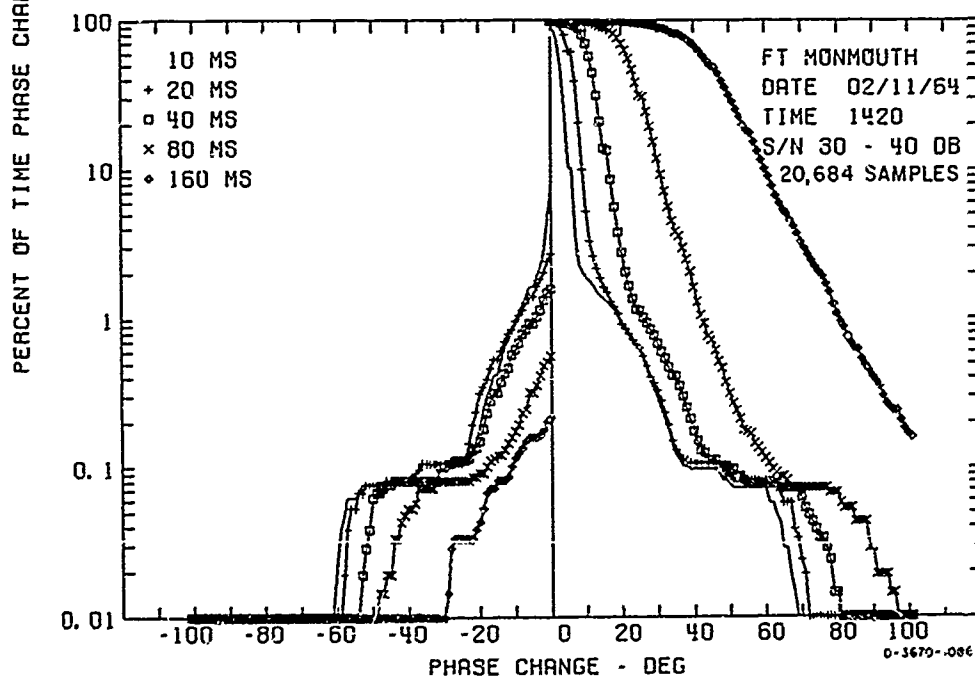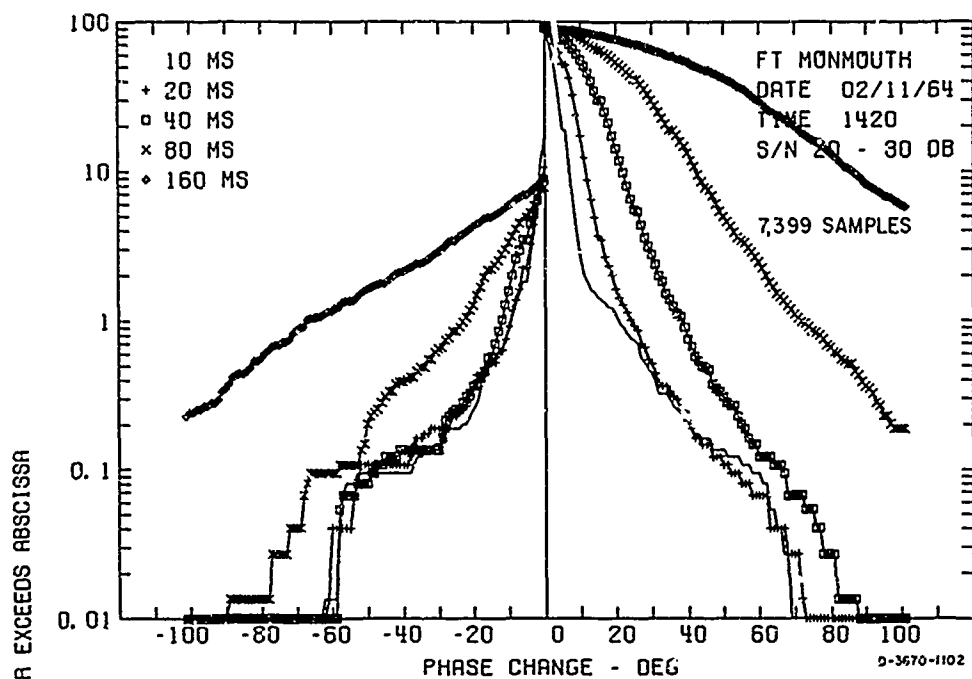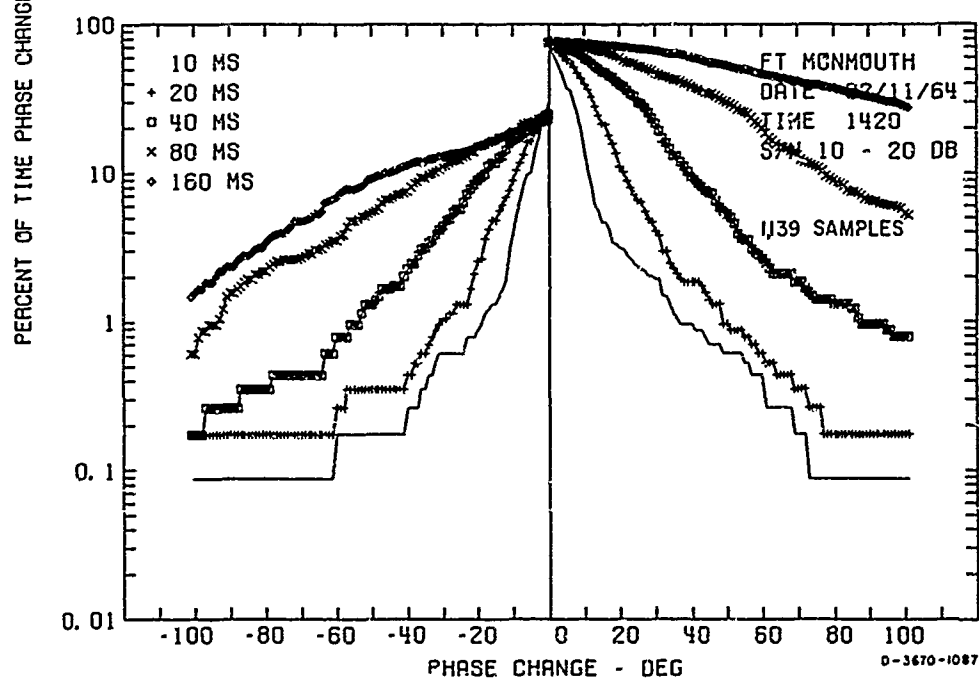

FIG. 15(d) PHASE DISTRIBUTION (S/N 10–20 db) — FORT MONMOUTH
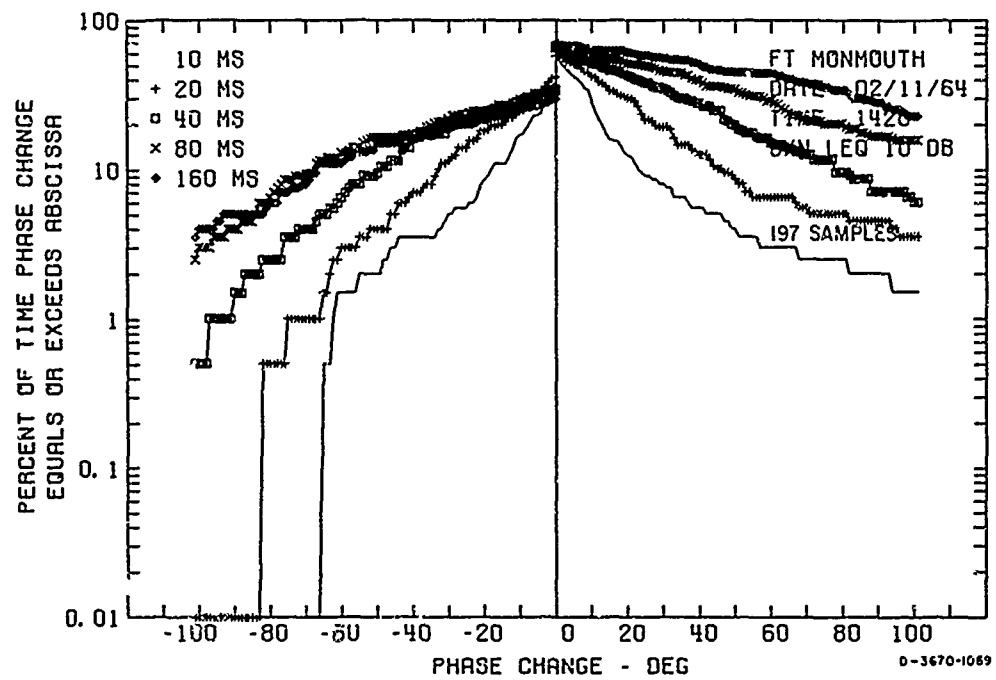1420 GMT, 11 FEBRUARY 1964

30

FIG. 15(e)   PHASE DISTRIBUTION (S/N < 10 db) — FORT MONMOUTH 1420 GMT
11 FEBRUARY 1964

Therefore, positive phase shifts greater than 45°/40 msec occurred
7399/29996 X 0.47 percent or 0.116 percent of the time during the
entire 5-minute period.

Figures 16(a) through 16(c) show the same type of plot for
the Thule transmission. Only three plots were compiled due to the low
signal-to-noise ratio. These three plots contain 29,994 samples.

d. Power Spectrum Plots

Power spectra of the received phase-stable signal can be useful
for computing error rates for FSK[3] and DPSK.[4] Models for error-rate
determination require measurements of frequency and time distortion.
The power spectrum shows frequency dispersion of the signal caused by
layer movement and changes and irregularities in electron density. The
mathematics for the computation of the power spectrum are given by Daly[8]
and will not be treated here. Examples of power spectra from both
paths are presented.

The power spectrum program computes the percent of the total
power within frequency intervals of 1/40 cps between ±10 cps of the
received carrier frequency. Often only ±3 cps is shown. Spectrum plots
show the percentage of received power shifted by various amounts in
frequency by reflections from the ionospheric layers. The plot's 0-cps
is the carrier frequency of 7,366,000 cps.

Power spectra for 5 consecutive minutes of the Fort Monmouth
signal are shown in Figs. 17(a) through 17(e). Examination of the
ionogram taken by the sounder on the path at this time showed that the
main modes contributing to the received signal were the 2F and the
3F. These modes correspond respectively to the two large spikes on the
spectrum plots at about +0.49 cps and +0.9 cps. The power spectrum plots
show the power received from the 2F and 3F modes varies from minute to
minute. Power is represented by the area of the spike and not by its
height alone.

The smaller peaks or lumps on the plots are probably due to
weak higher-order modes, which are not observable on the ionogram. It
is possible that the peak between the 2F and the 3F, which increases

32
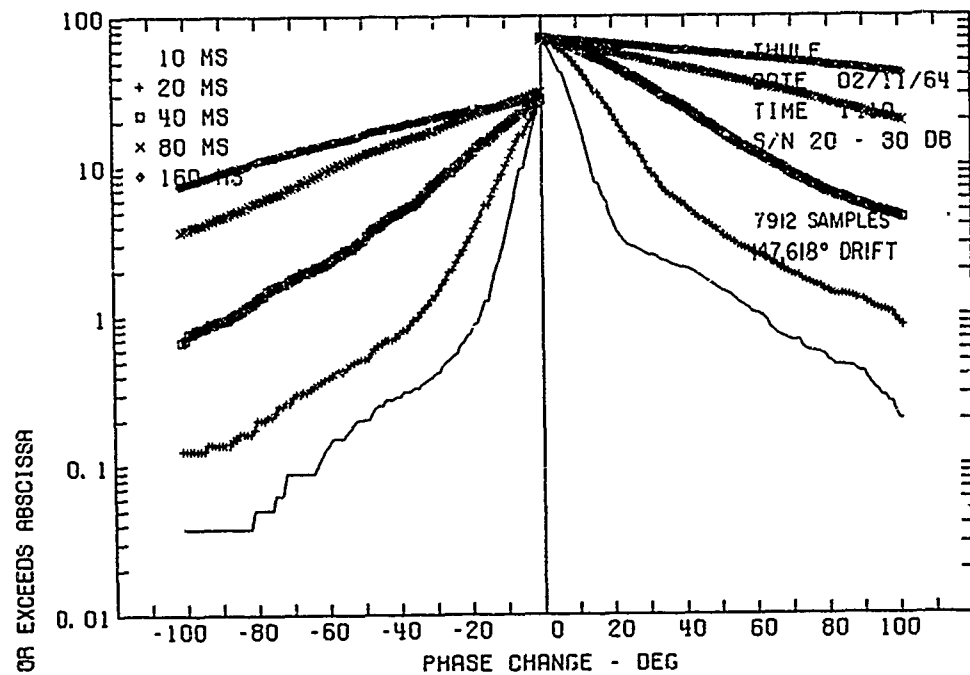
FIG. 16(a)   PHASE DISTRIBUTION (S/N 20–30 db) — THULE 1410 GMT,
            11 FEBRUARY 1964
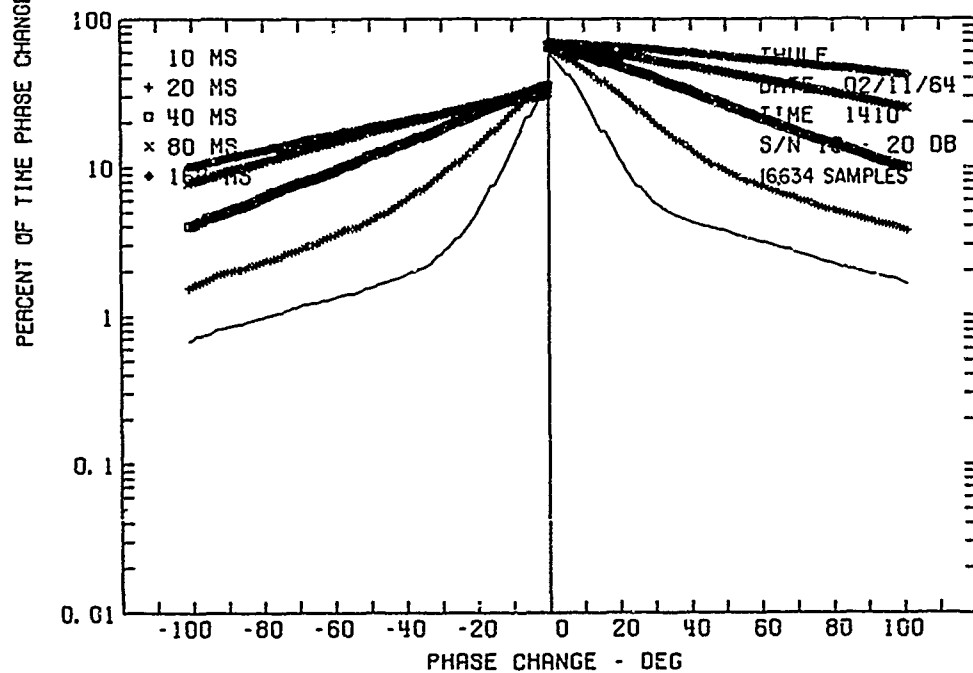
FIG. 16(b)   PHASE DISTRIBUTION (S/N 10–20 db) — THULE 1410 GMT,
            11 FEBRUARY 1964

33
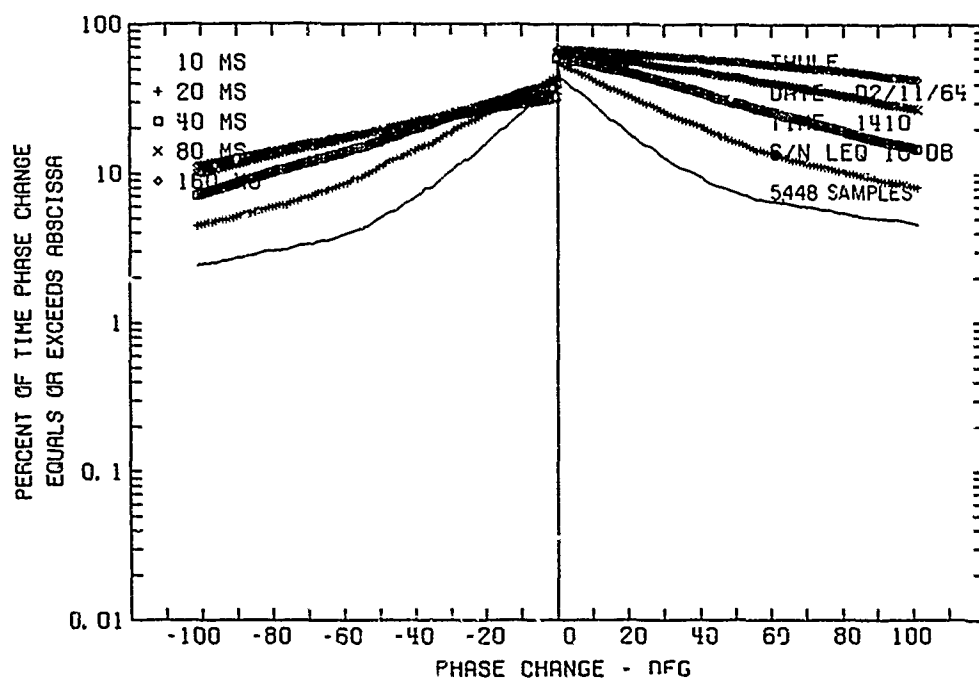
FIG. 16(c)   PHASE DISTRIBUTION (S/N < 10 db) — THULE 1410 GMT,
11 FEBRUARY 1964

34
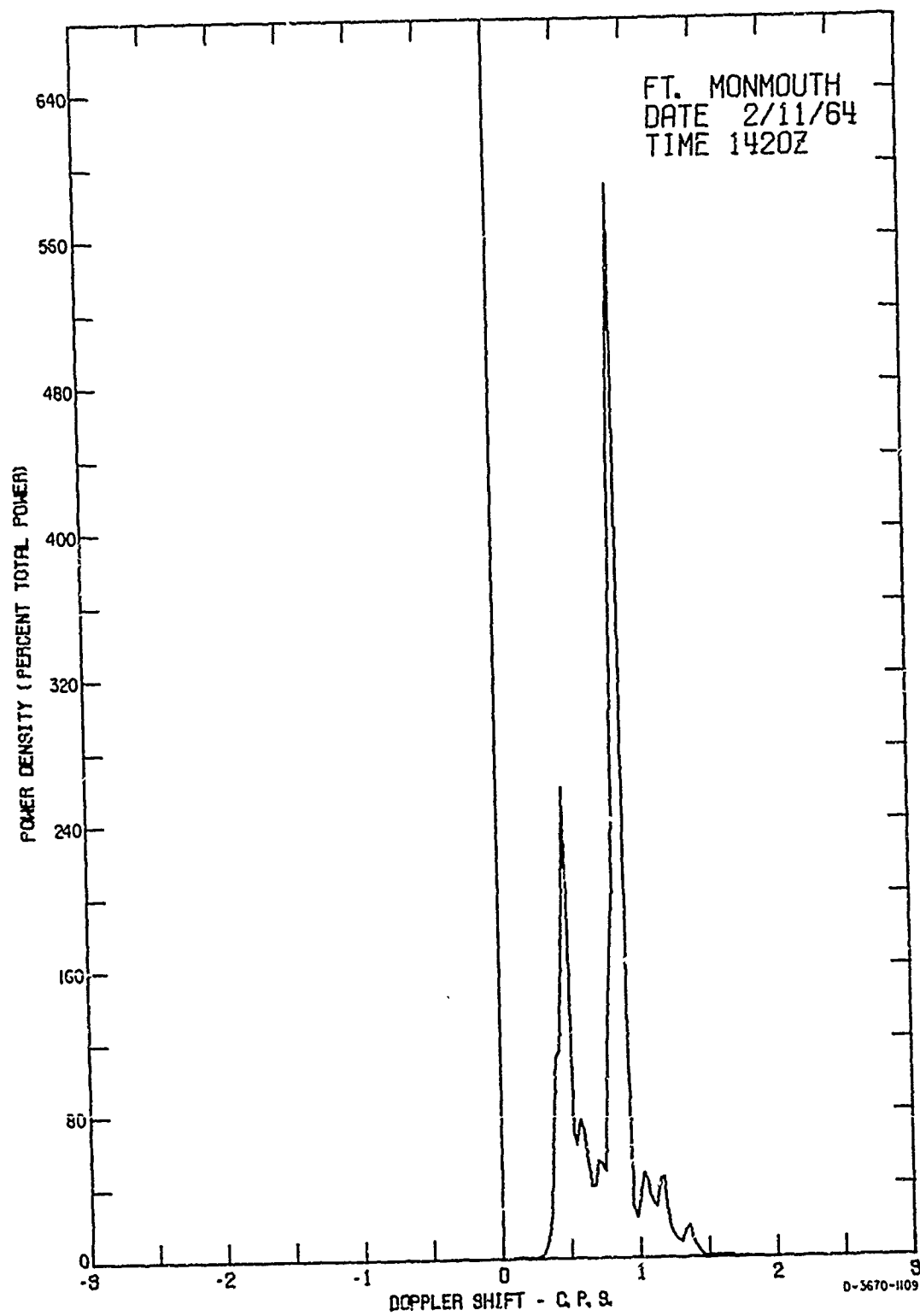
FIG. 17(a) POWER SPECTRUM — (FORT MONMOUTH) 1420 GMT, 11 FEBRUARY 1964
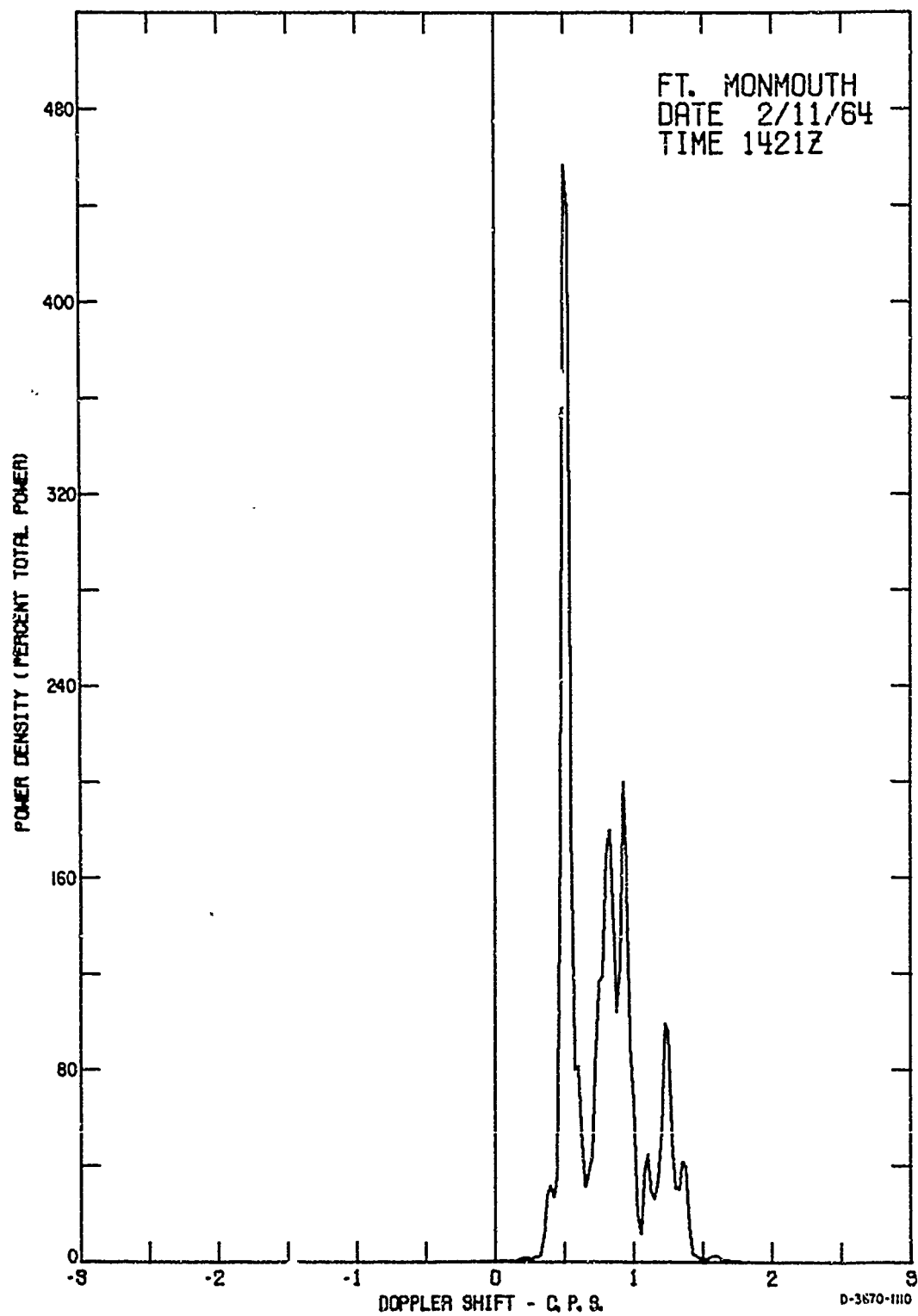
FIG. 17(b)   POWER SPECTRUM — (FORT MONMOUTH) 1421 GMT, 11 FEBRUARY 1964

36
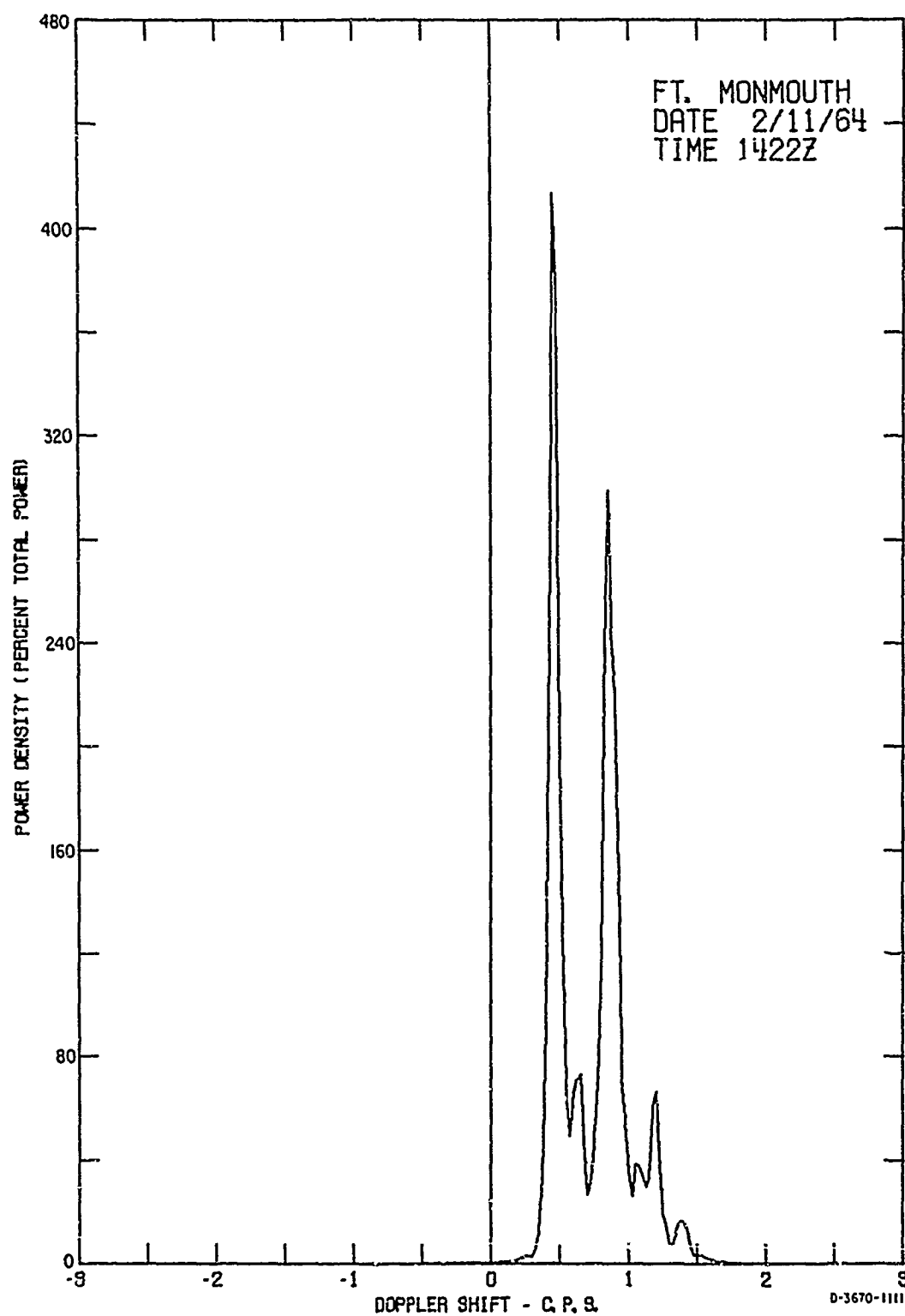
FIG. 17(c) POWER SPECTRUM — (FORT MONMOUTH) 1422 GMT, 11 FEBRUARY 1964

37
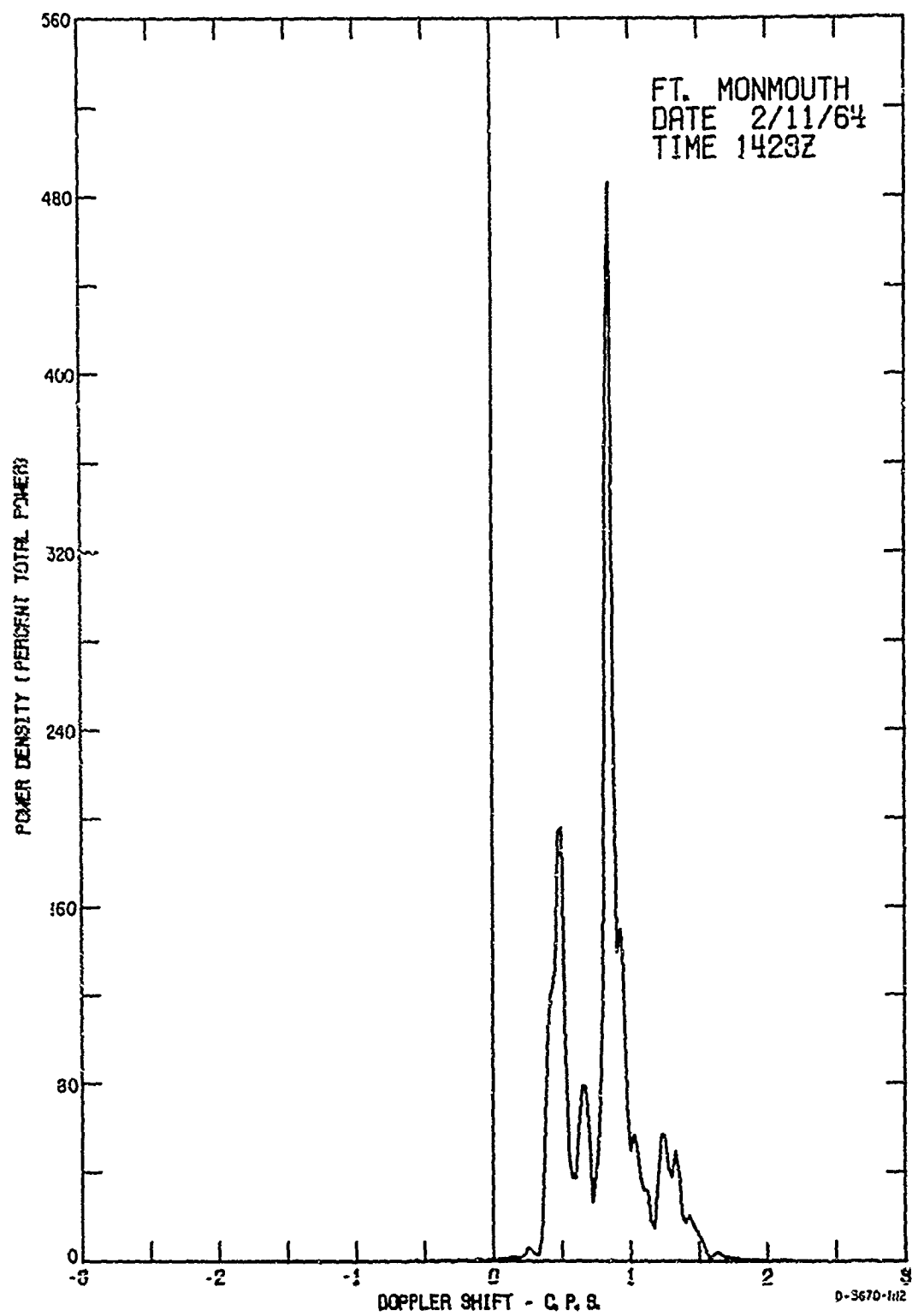
FIG. 17(d)   POWER SPECTRUM — (FORT MONMOUTH) 1423 GMT, 11 FEBRUARY 1964

38
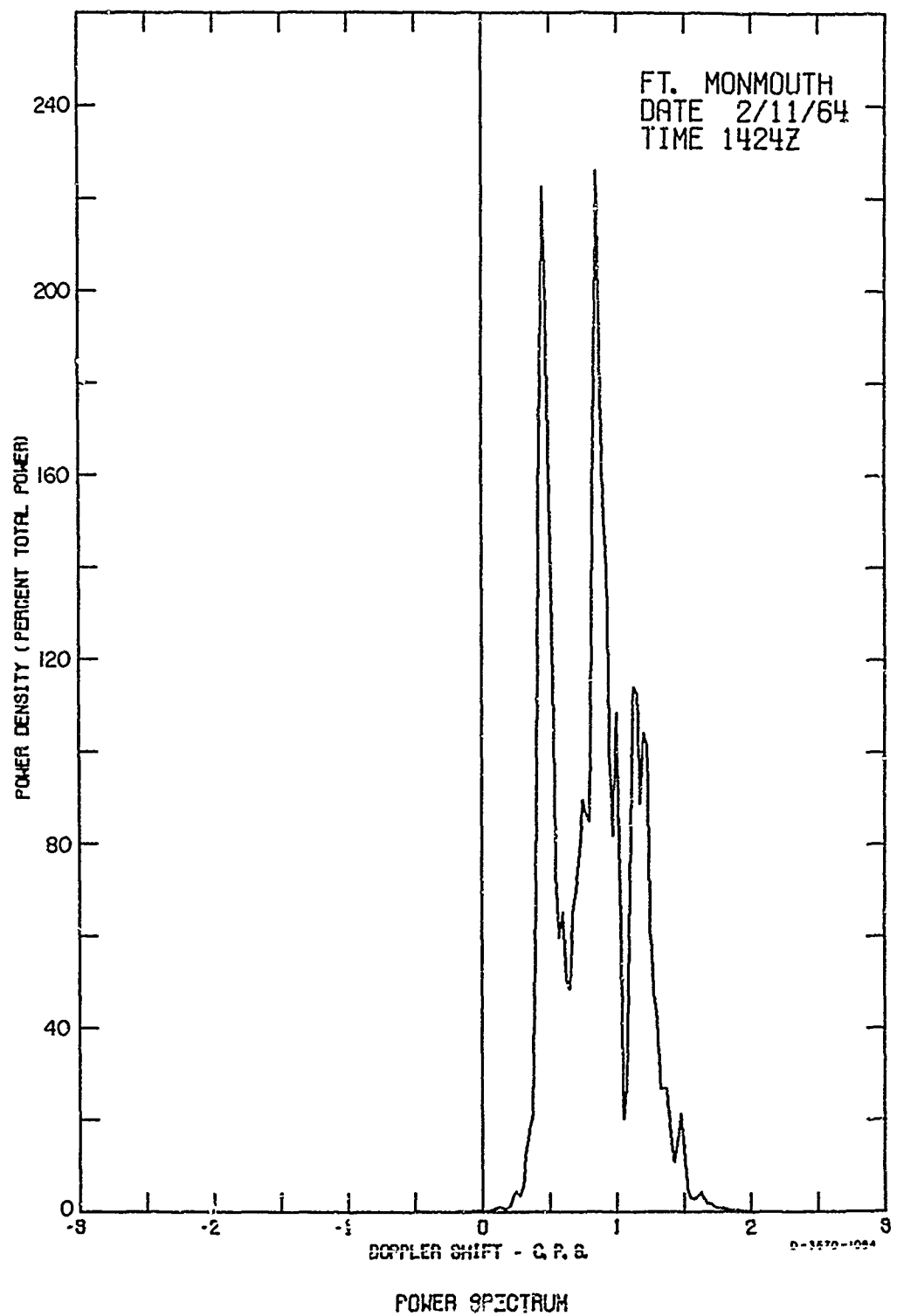
FIG. 17(c)   POWER SPECTRUM — (FORT MONMOUTH) 1424 GMT, 11 FEBRUARY 1964

greatly in relative amplitude in the 1421Z spectrum, is a complex mode, as its Doppler shift is between that of the 2F and the 3F. At this time of day (1420 GMT or 0620 PST) the Doppler shift is positive as the ionosphere drops and the mode paths become shorter. Assuming a height for the F layer of 250 km, the layer height rate of change computed from each mode's Doppler shift indicates that the F layer was falling at about 15 meters per second in the first 2 minutes and about 15.5 meters per second in the last 3 minutes.

The power spectrum for one minute of the Thule signal is shown in Fig. 18. The Thule signal is spread from about 4 cps below the transmitted frequency of 7.366 Mc to about 6 or 8 cps above, whereas the Fort Monmouth signal was spread only from about 0.3 cps to 1.4 cps. This spreading is typical of the Thule to Palo Alto path, which passes through the auroral zone. This spectrum indicates the presence of many modes, each with its own Doppler shift. Ionograms for the Thule path usually have a spread appearance, unlike the clean modes which are associated with the Fort Monmouth path.
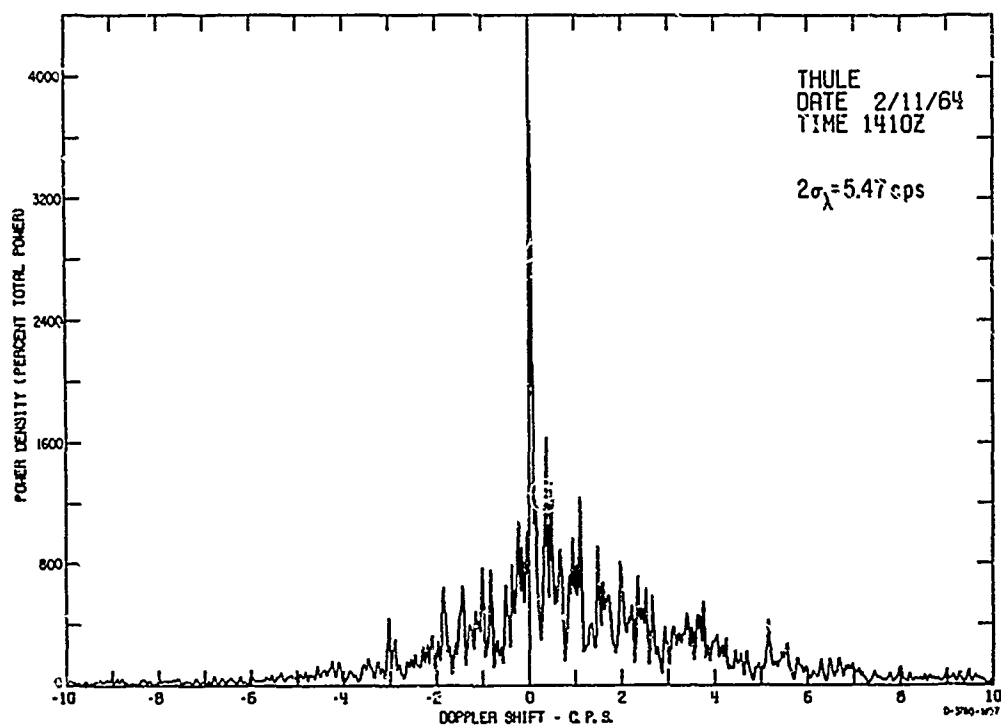
FIG. 18 POWER SPECTRUM — (THULE) 1410 GMT, 11 FEBRUARY 1964

41

III   SYSTEM TESTS AND FREQUENCY ACCURACY

A.   TEST OBJECTIVES

In order to determine the accuracy and reliability of the receiving
and data processing system, data from several controlled-input tests
have been reduced to plot form. By accurately controlling the input
signal into the data collection system, errors induced by the various
portions of the receiving and processing system can be identified and
estimates of resolution made.

1.   Stable Phase and Amplitude Test--Receiver Excluded

The first of these controlled-input tests (Test 5001) was conducted
to determine the resolution of the receiving system exclusive of the
receiver itself. The test was made by connecting batteries to the
AMPLITUDE and PHASE inputs of the tape recorder. This action removed
the receiver and any possible variable signal source from the data col-
lection system; consequently, Figs. 19 through 22 illustrate only
errors induced by the record and playback analog tape recorders and by
the computer data processing programs. The battery voltage for the
AMPLITUDE channel was equivalent to an input signal of about 64 db above
1 μv; the voltage for the PHASE channel to a phase angle of about 90°.

The amplitude density plots of Figs. 19 and 20 should show narrow
spikes at very high percentage of occurrence since the amplitude of the
signal should be invariant. The slight spreading and lowering of the
spikes can be attributed to the record and playback tape recorders. A
plot of the amplitude distribution shows that the signal is within
± 1 db of its median value about 98 percent of the time. The standard
deviation σ, of the signal plus noise is about 0.3 db. According to the
manufacturer's specifications, the signal-to-noise ratio of the recorder
for maximum rms signal (that is, the peak values of the signal are at max-
imum frequency deviation) to rms noise at center carrier at 3-3/4 ips is
40 db. Center carrier for the tape recorder corresponds to a receiver

43
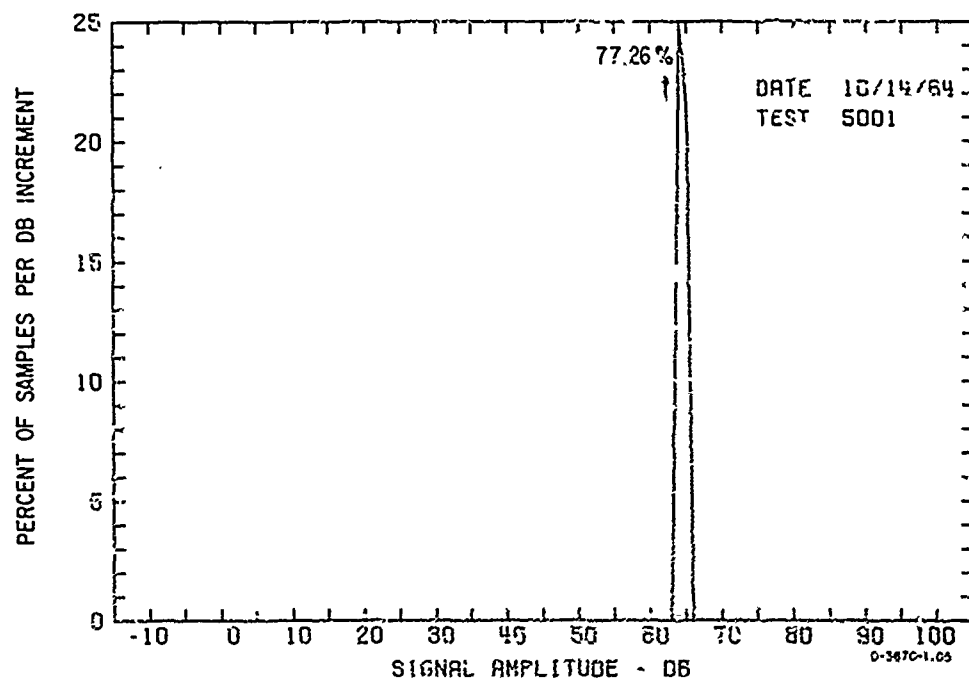
FIG. 19 AMPLITUDE DENSITY (db) — STABLE PHASE AND AMPLITUDE
TEST (5001)
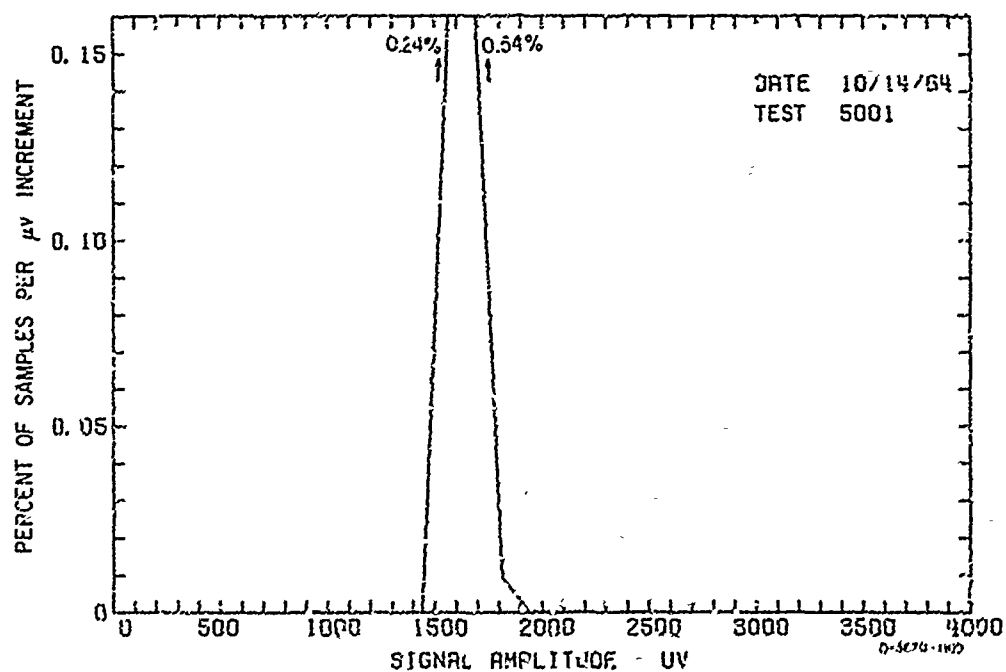
FIG. 20 AMPLITUDE DENSITY (μv) — STABLE PHASE AND AMPLITUDE
TEST (5001)

input signal about 50 db below that which causes maximum rms frequency deviation, so the rms noise could be expected to be about 40 db down from this maximum, or about 50 X 0.01 or 0.5 db. If band-limited noise statistics are applicable, we would then expect that the probability of the signal plus noise being within ±1 db of the mean would be 95 percent. Therefore, the figure of signal variation within ±1 db 98 percent of the time is within the specifications of the tape recorder, and the amplitude spreading is attributable to the internal noise of the tape recorder.

Figure 21 shows the phase-change plot. Since the phase change should be zero, it can be seen that an error of 3° or more per time interval will occur only about 1 percent of the time. Center frequency on the phase channel corresponds to a phase angle about 100° below the angle which causes maximum rms frequency deviation, so the rms noise, according to the manufacturer's specification, is equivalent to 1.0^o. The standard deviation of the phase-change distribution is about 1.1^o. It appears that both the AMPLITUDE and the PHASE channels
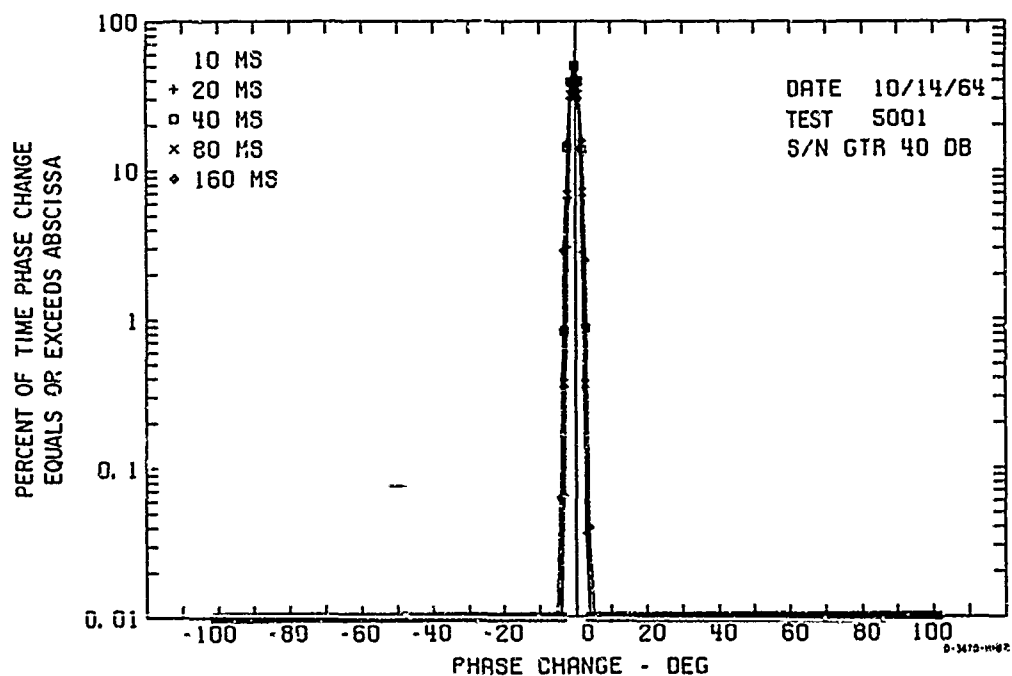
FIG. 21 PHASE DISTRIBUTION (S/N > 40 db) — STABLE PHASE AND AMPLITUDE TEST (5001)

45

have better signal-to-noise ratios than the manufacturer's specifications would indicate, even though the data used in the comparison were somewhat contaminated by noise inherent in the sampling and quantizing process.

A characteristic of the power spectrum program is that (since the signal is not sampled for an infinite time) even stable-frequency signals are plotted as having some width. Daly[8] shows the resolution of the program itself by simulating data possessing tones of 1 and 3 cps. As a measure of the resolution, his spikes can be approximated as triangles, and if this is done, then their base width is about 0.111 cps and we can never hope to realize a narrower spike. Frequency-stable signals at the carrier frequency are not plotted, because the program's inherent spread would make it misleading to do so. Instead, the amount of power exactly at the carrier frequency is given in printout form, and a continuous curve of the ac power may be drawn through the carrier frequency (0 cps) to show continuity of Doppler shifts only slightly above and below the carrier frequency.

The power spectrum for Test 5001 (Fig. 22) has a very large power component at the carrier frequency since the stable phase was simulated with a battery. This on-frequency component, which amounts to 99.69 per-cent of the total power, is not shown, and the figure indicates only an exaggerated view of the 0.31 percent of the total power which is offset in frequency by tape recorder variations. The tape recorder-induced wow or flutter component of about 1.75 cps can be seen on this spectrum. The power contained in this flutter component is so low in comparison with the power of the received data signal that it is detect-able only on special tests and is not seen on other spectrum plots.

Figures 19 through 21 show that noise is introduced by the tape recorder in both the AMPLITUDE and the PHASE channels. Since both effects are occurring, the apportionment of the noise contribution between the two, as observed in the power spectrum of Fig. 22, is very difficult. It is not known which is the greatest contributor to the noise.

46

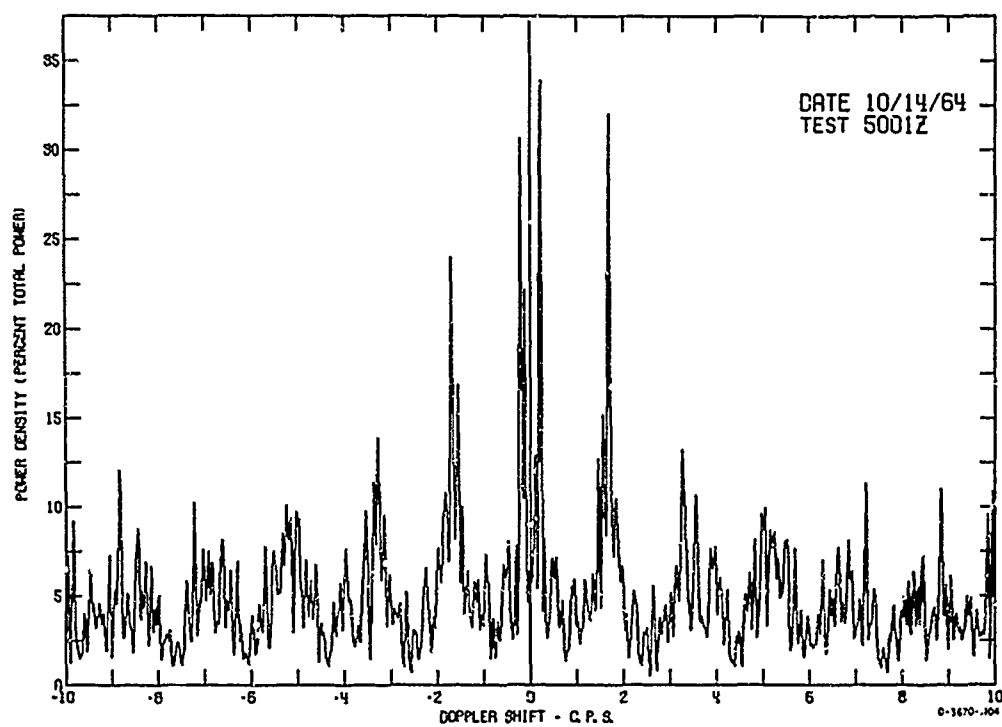FIG. 22   POWER SPECTRUM — STABLE PHASE AND AMPLITUDE TEST (5001)

47

2. Stable Phase and Amplitude Test--Receiver Included

Controlled-input tests 5002 and 5003 are similar in purpose to
Test 5001 except that the receiving system itself is also examined under
conditions of stable phase and amplitude. These two tests use as an
input to the receiver a 7,366,000-cps phase-stable signal from a Rohde
and Schwarz XJA Frequency Synthesizer. The synthesizer was operating
with its frequency locked to the local frequency standard. Therefore,
there should be no phase drift. The signal levels into the receiver
were at about 60 db and 20 db above 1 μv for Tests 5002 and 5003,
respectively. This allows comparison of receiver noise effects at two
signal levels.

Figure 23, the amplitude density for the 60-db signal, is not sig-
nificantly different from Fig. 19, indicating that at least at this
high signal level, the receiver-frequency synthesizer combination does
not add noise beyond that referred to in Test 5001. The standard devia-
tion,σ, of the 60-db signal plus noise is estimated at about 0.4 db.
Figure 24 shows the amplitude-spreading effects of the lower, 20-db,
signal level. For this test, the signal plus noise is within ± 1.7 db
of the median signal of 22.2 db 98 percent of the time. The signal
plus noise 's within ± 1.0 db of the median only about 84 percent of the
time. The standard deviation,σ, of the 20-db signal plus noise is about
0.7 db. This means that with the 60-db signal, the receiver has added
noise sufficient to spread the standard deviation of the signal plus
noise an additional 0.1 db beyond the figure of Test 5001. With the
20-db signal, the increase in σ is, of course, greater.

The phase-change plots of Figs. 25 and 26 are shown for comparison
with Fig. 21 and with each other. Since the first plot was made with
the same high signal level as in Test 5001, it is interesting to note
that the phase change is certainly no greater than when the receiver
was not included. The receiver-frequency synthesizer combination added
no noticeable phase noise over that determined in Test 5001 to be
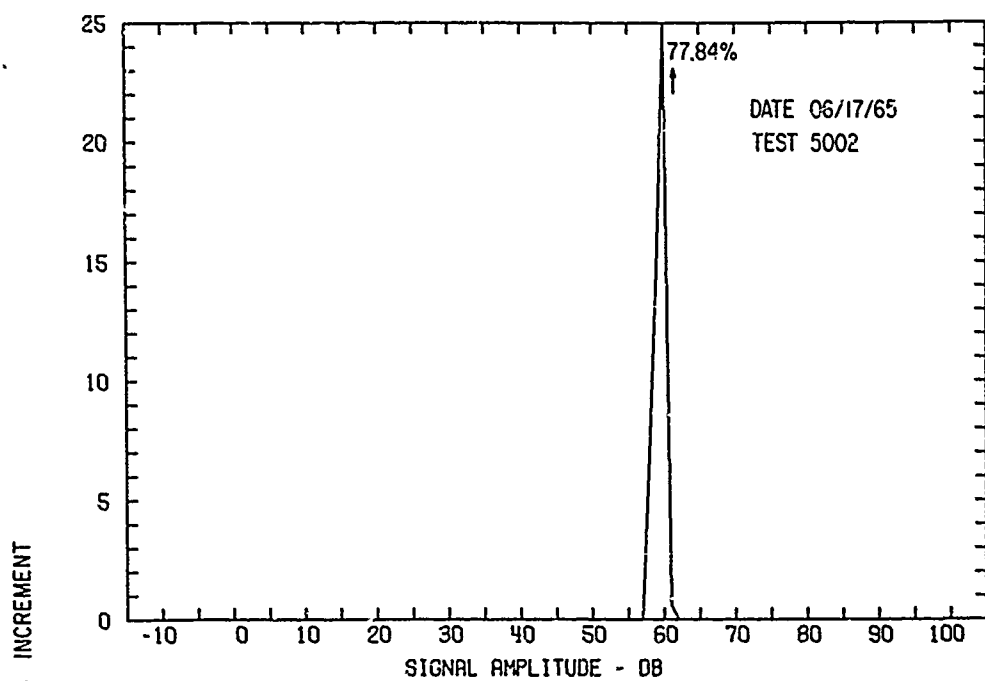caused by the tape recorders.

48

FIG. 23 AMPLITUDE DENSITY (db) — STABLE PHASE AND AMPLITUDE TEST (5002)
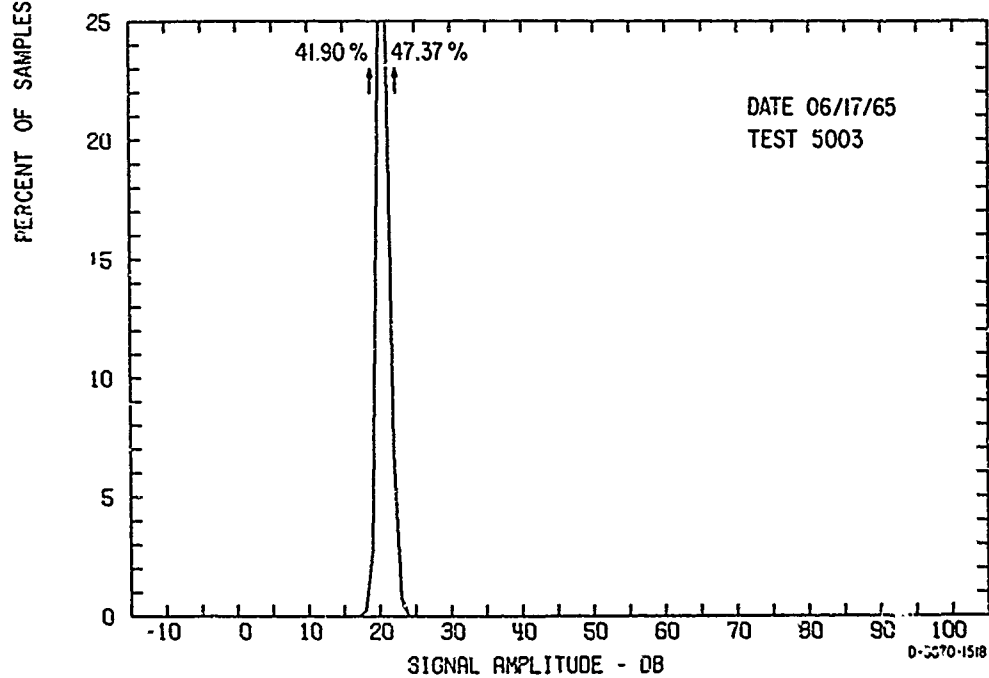

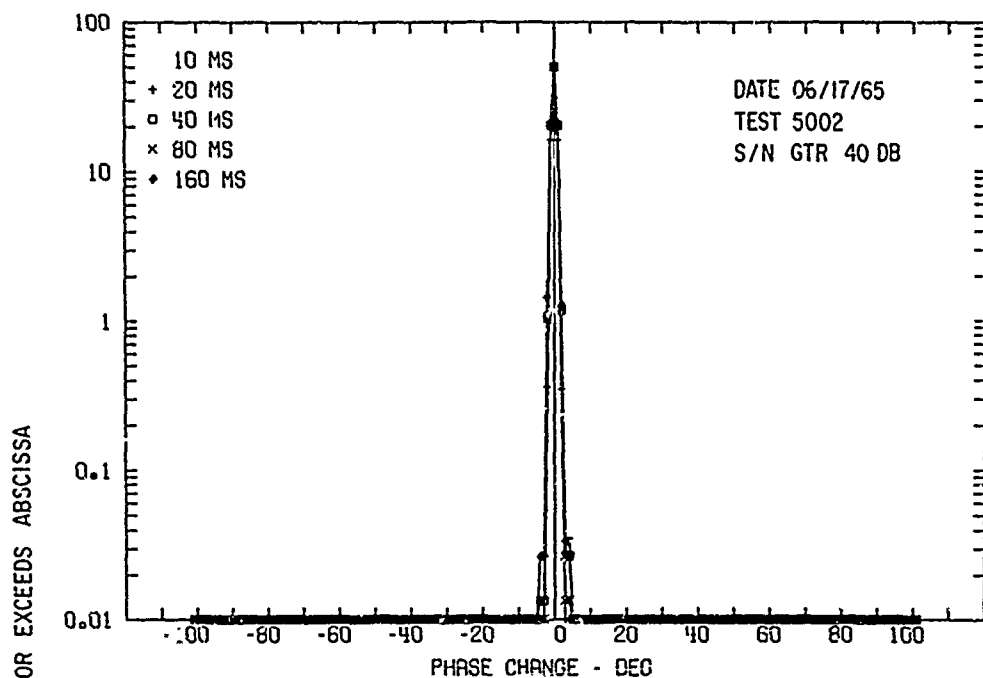FIG. 24 AMPLITUDE DENSITY (db) — STABLE PHASE AND AMPLITUDE TEST (5003)

49

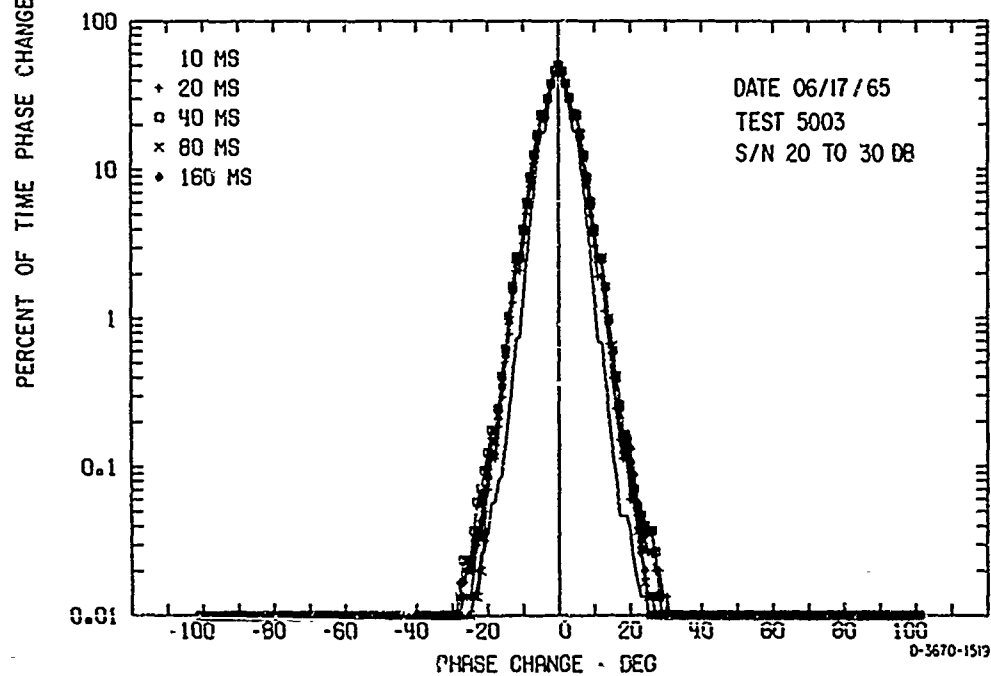FIG. 25 PHASE DISTRIBUTION — STABLE PHASE AND AMPLITUDE TEST (5002)

FIG. 26 PHASE DISTRIBUTION— STABLE PHASE AND AMPLITUDE TEST (5003)

50

Test 5003 (Fig. 26) shows that for the 20-db signal level, this is certainly not so. Evidently at this signal level, approximately 40 db down from the high level, the phase noise is appreciable. In fact, the probability of a phase change of 3 degrees or more increases by a factor of about 1500 from about 0.02 percent of the time to about 30 percent of the time. This plot reflects the randomness of the phase of the receiver noise, which is of much greater consequence when the signal is of the order of 20 db above 1 μv rather than about 60 db. Positive and negative phase changes occur with approximately equal probability. Since the curves for all time intervals with the exception of the 10-msec interval are superimposed, it is evident that the phase changes are rapid and random. For a given phase change, the 10-msec curve shows a lower probability of occurrence. This is probably the result of the system not being capable of responding to some of the more rapid phase changes in as short a time as 10 msec.

The spectrum plot for Test 5002 (Fig. 27) shows the same sort of tape-recorder-induced spikes as does Fig. 22, although their spacing is not the same. Another noticeable effect on this spectrum is the dispersion of the signal in the immediate vicinity of the oscillator frequency, but far enough off that it is plotted as off-frequency power. This is probably caused by the noise of the receiver-frequency synthesizer combination. Figure 22 did not display this effect. Figure 27 shows only 0.13 percent of the total power, the remaining 99.87 percent being the on-frequency component.

When the signal level was decreased about 40 db for Test 5003, the percent of on-frequency power dropped to 98.81 percent of the total power, and the tape recorder spikes became obscured in the noise. Still apparent in Fig. 28, however, is the signal which is just off zero Doppler shift. This spectrum shows only part of the 1.19 percent of the total power which is off-frequency. Since it appears that the noise signal is not decreasing near the edges of the window ±10 cps about zero Doppler shift, it can be concluded that this is an approximation to white noise and that it extends in frequency until attenuated by the bandpass filters.
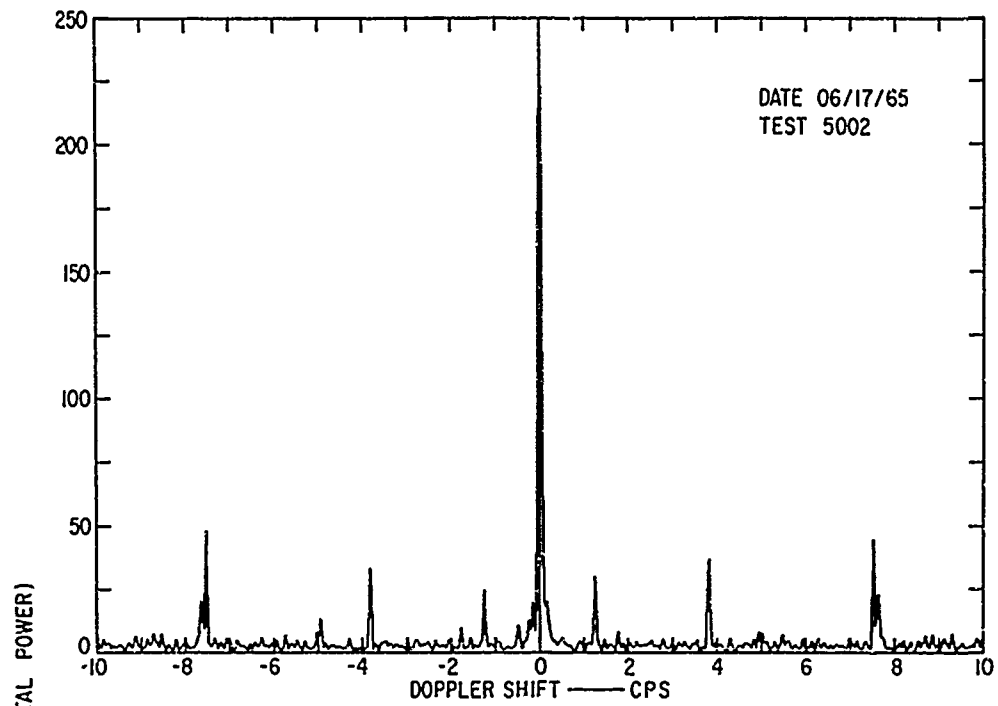
51

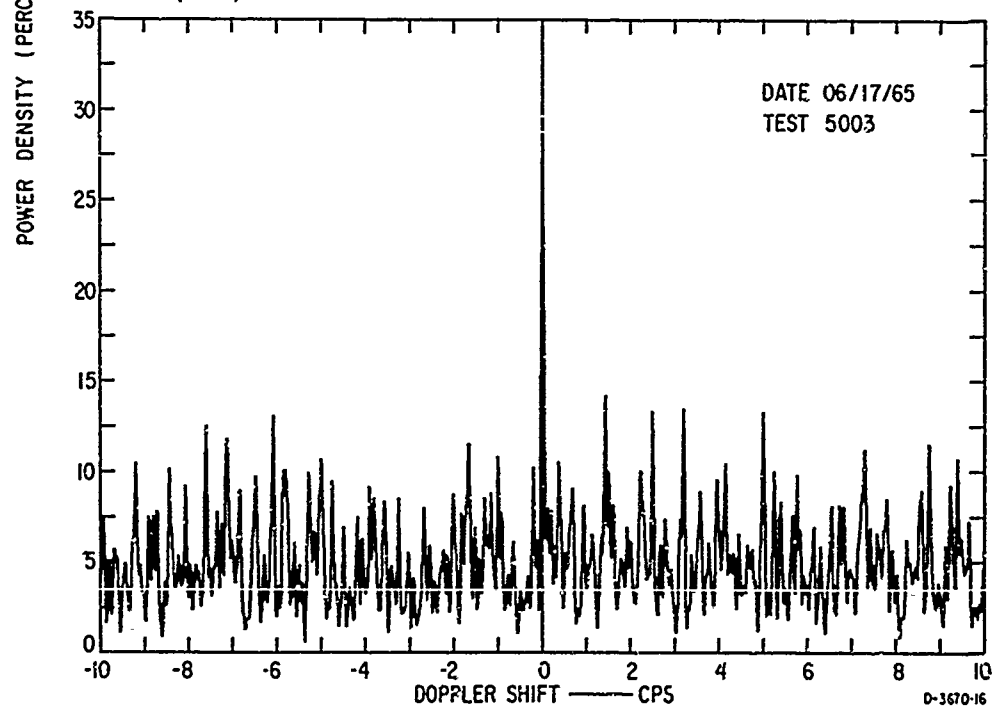FIG. 27 POWER SPECTRUM — STABLE PHASE AND AMPLITUDE TEST (5002)

FIG. 28 POWER SPECTRUM — STABLE PHASE AND AMPLITUDE TEST (5003)

3. Stable Frequency and Amplitude Test

With the available system resolution from the previous test known, it is interesting to estimate the effects of the receiver by another study. In this stable frequency and amplitude test (Test 5102), the system is evaluated on other than a phase-stable signal.

The amplitude of the input signal was set to about 62 db above 1 μv ar the frequency was offset about -0.65 cps to 7,365,999.35 cps. A Rohde-Schwarz Model XUA Frequency Synthesizer was used to generate this input. This synthesizer will lock on to an external frequency standard at 1-kc intervals but uses its own internal standard for other frequencies. The frequency drift of this standard is approximately 5 parts in 10^8 per day. The input signal simulates a single mode with no fading effects but with constant upward layer movement. The signal could be represented by a vector of constant amplitude and rotation rate.

Figures 29 and 30 are the amplitude-density plots for this signal. As was the case with Test 5002, the plots are both somewhat wider than those shown in Figs. 19 and 20, due in part to the added factor of receiver noise. The amplitude distribution, Fig. 31, on probability paper, shows that the output is normally distributed about a mean of 62.2 db with a standard deviation, σ, of 0.6 db. In this test, the addition of the unlocked frequency synthesizer caused the amplitude data to be spread so that 86 percent of the data fell within ±1.0 db of the mean; 98 percent fell within ±1.5 db of the mean. This is very similar to the results of Test 5003.

Another characteristic of Test 5102, in addition to the constant input signal amplitude, was the steadily decreasing phase angle, from which the phase angle distribution of Fig. 32 is compiled. The plot would theoretically contain a set of curves indicating only negative phase change. Since the phase drift was about -0.65 cps, the 160-msec curve should indicate a maximum phase shift of $0.65 \times 360 \times 160/1000$ = $-37.5°$ 100 percent of the time, then abruptly drop to 0 percent for greater negative shifts. The 80-msec curve should indicate $-18.75°$; the 40-msec curve $-9.37°$, etc.
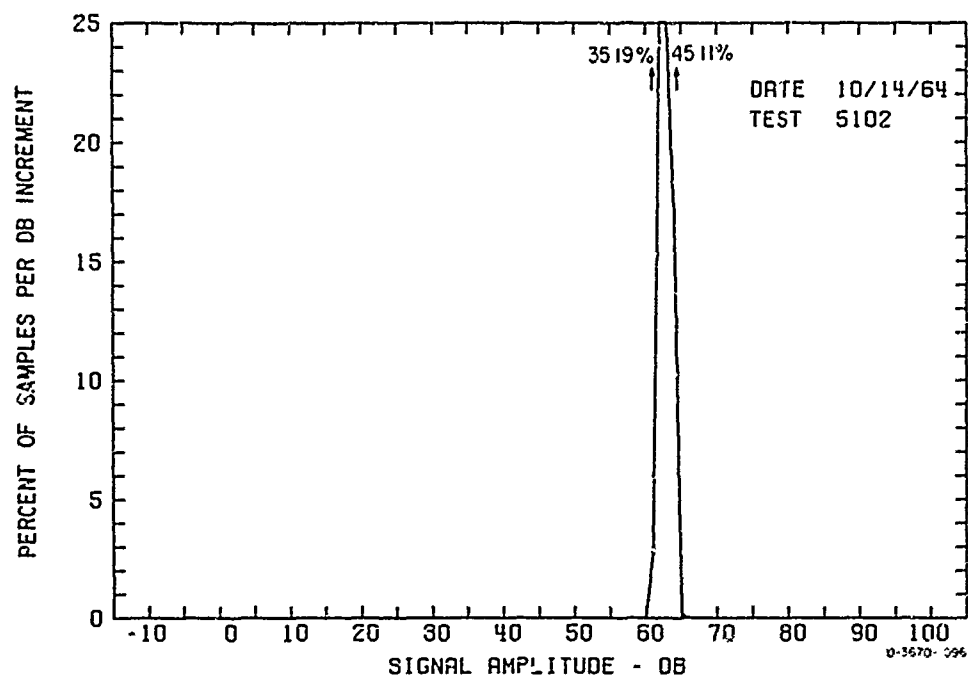
FIG. 29 AMPLITUDE DENSITY (db) — STABLE FREQUENCY AND AMPLITUDE
TEST (5102)
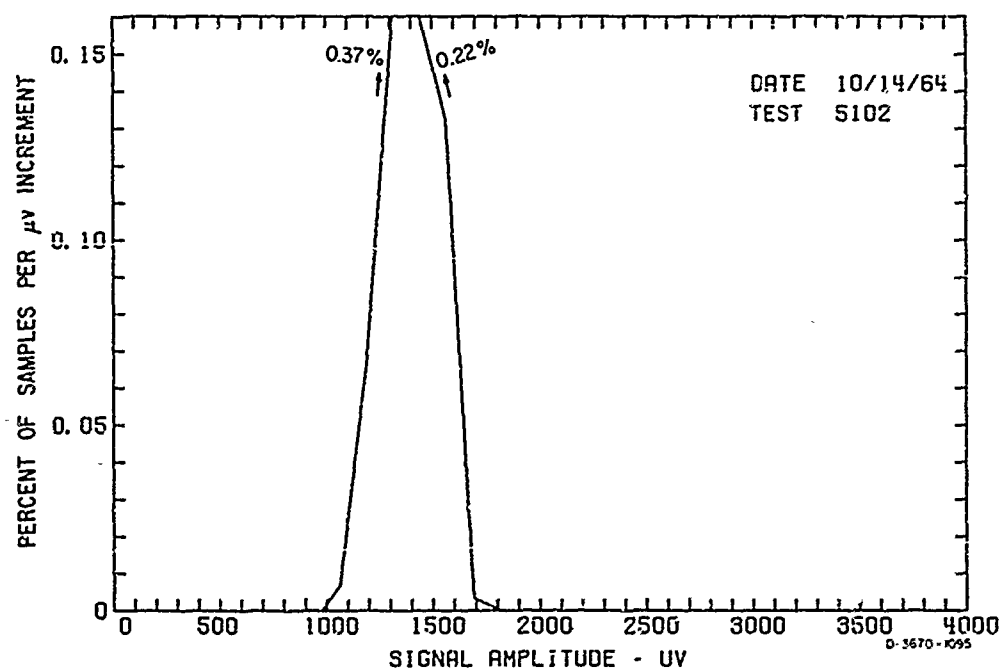
FIG. 30 AMPLITUDE DENSITY (μv) — STABLE FREQUENCY AND AMPLITUDE
TEST (5102)

54
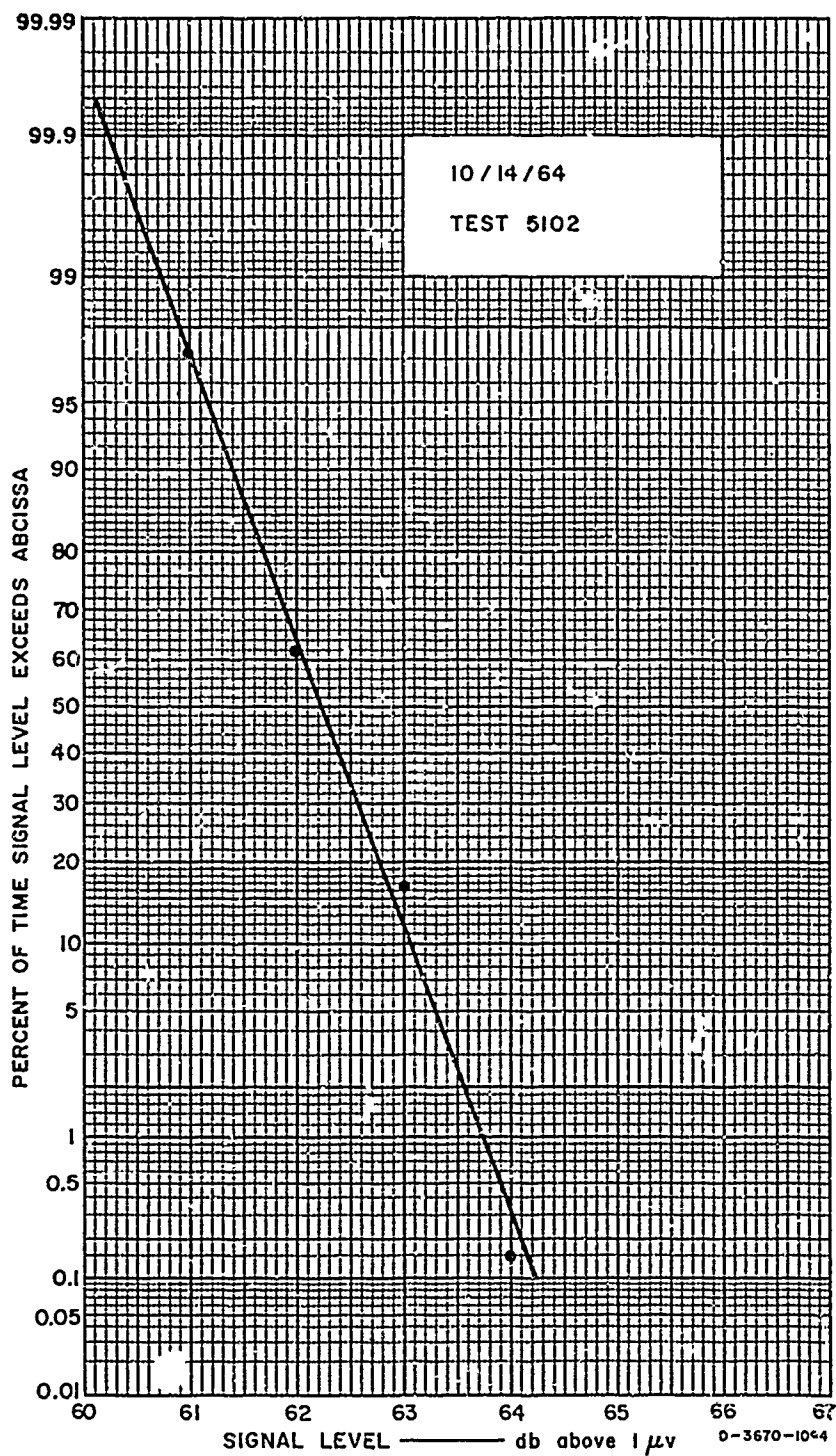
FIG. 31 AMPLITUDE DISTRIBUTION — STABLE FREQUENCY
AND AMPLITUDE TEST (5102)
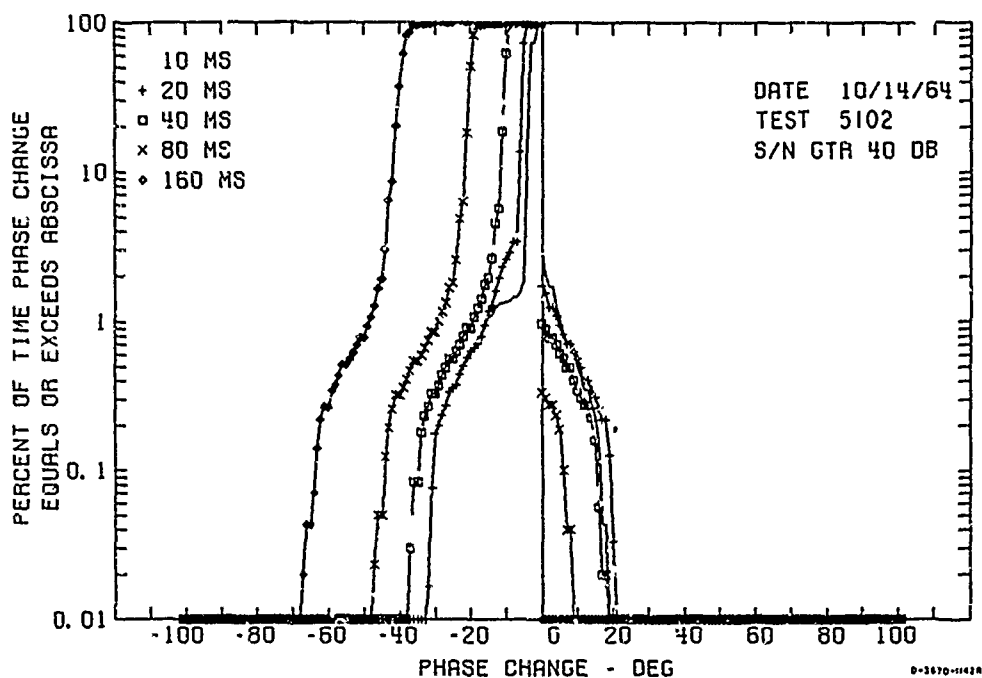
FIG. 32 PHASE DISTRIBUTION (S/N > 40 db) — STABLE FREQUENCY
AND AMPLITUDE TEST (5102)

Two types of deviation from the expected behavior are apparent;
the curves do not drop vertically on the negative side and some positive
values of phase change exist. These discrepancies cannot be accounted
for by the long-term stability of the synthesizer's internal standard,
which is quoted at about 5 parts in 10^8 per day. This standard would
allow a change in the drift of only about 0.07 degrees per 160 msec
during the 5-minute period. The previous tests indicated that tape
recorder noise and receiver noise (at this high signal level) are not
sufficient to account for this discrepancy. There were, in the digitizing
process, no occurrences of either amplitude or phase voltages which
exceeded the digitizer limits, so it must be concluded that tape dropouts
did not occur.

This leaves the non-locked frequency synthesizer and the phase
distribution computer program itself. The phase extrapolation process
described in Sec. II-C-1-c of this report is a possible source of error

56

in a test of this sort, since the extrapolated phase values may differ
by a few degrees from the theoretically linear phase vs. time relation-
ship of this special test. Furthermore, although Test 5002 showed the
frequency synthesizer to be phase-stable when locked to an external stan-
dard, it is not known to what extent this phase stability still applies
when the synthesizer is not locked. Another possibility is that of dis-
turbances in line voltage during the test. Such disturbances have been
noticed in the past--usually due to the starting or stopping of air-
conditioning equipment--and they are known to cause transients in the phase
and amplitude output of the receiver. They may very possibly also cause
short-term variations in the output frequency of the frequency synthesizer.

The power spectrum shown in Fig. 33 shows one clean spike at
-0.65-cps, the frequency offset of the input signal from the carrier.
If this spike is approximated as a triangle, then its base width is
0.155 cps as compared with the best possible figure of 0.111 cps. From
this we can conclude that the receiver and frequency synthesizer together
resulted in only 0.155 minus 0.111 or 0.044 cps of frequency spreading
as measured in this manner. Actually, the plot shows several small
lumps near the bottom of the spike. These are almost certainly the
frequency deviations which are seen on Fig. 32.

4. Simulated Two-Mode Test

Test 5201 was designed to observe the behavior of the system in a
relatively realistic situation. This test simulates a signal propagated
by two modes of almost equal strength, one mode absolutely stable, the
other mode having a slightly positive Doppler shift, as would occur if
the reflection point for this mode were slowly dropping. This test was
conducted by injecting two HF signals into the receiver. One signal was
set to 7.366 Mc, the other about 0.05 cps high in frequency. The
two-mode situation was discussed in Interim Report 3.[1] The theoretical
amplitude and phase plots from Interim Report 3 are shown in Fig. 34(a)
for comparison with the actual chart paper recording made during the
test, as shown in Fig. 34(b). The theoretical waveform of Fig. 34(a)
labeled $A_1/A_2 \cong 1$ (approximately equal-strength modes) should be used

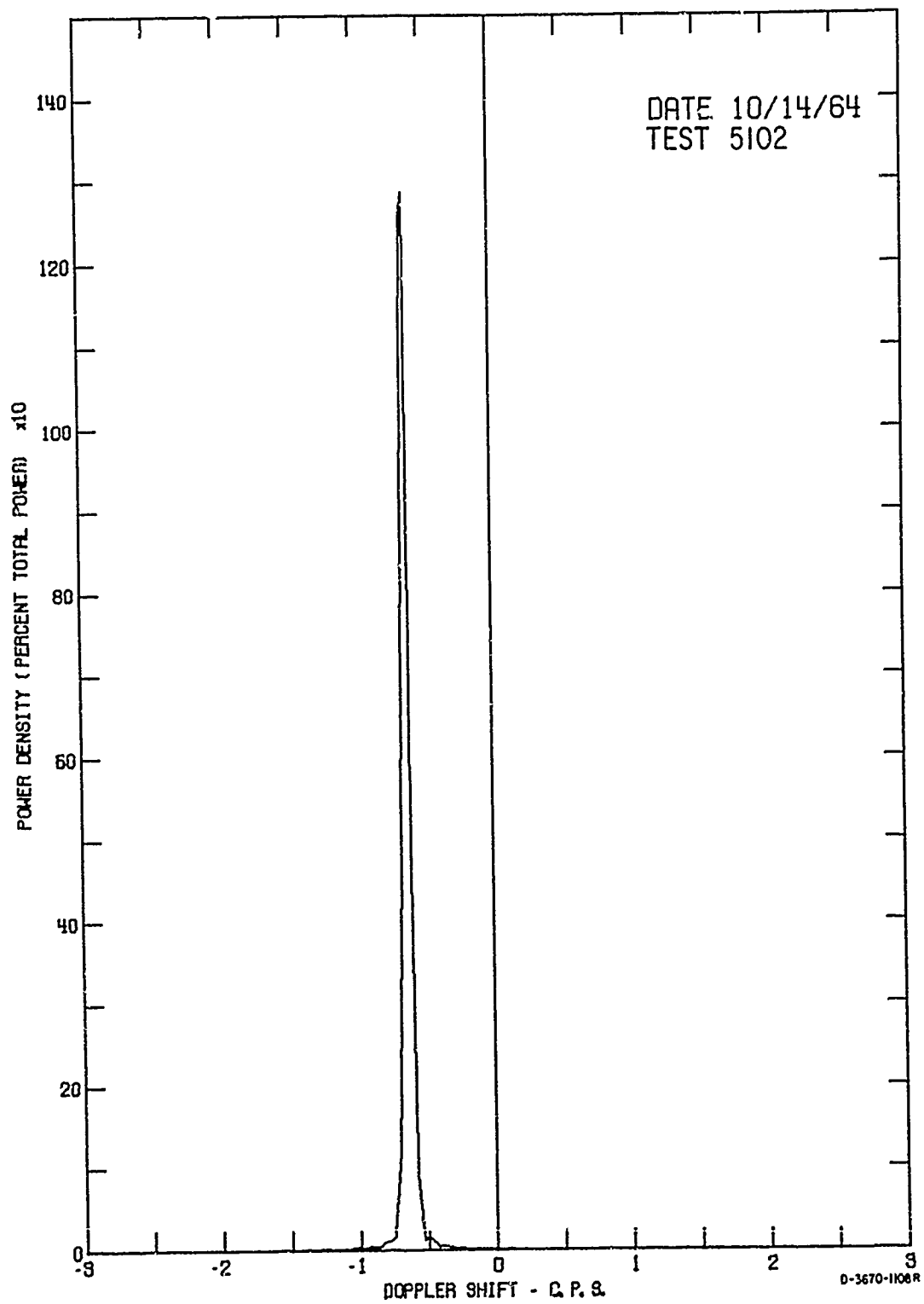57

FiG. 33 POWER SPECTRUM — STABLE FREQUENCY AND AMPLITUDE TEST (5102)
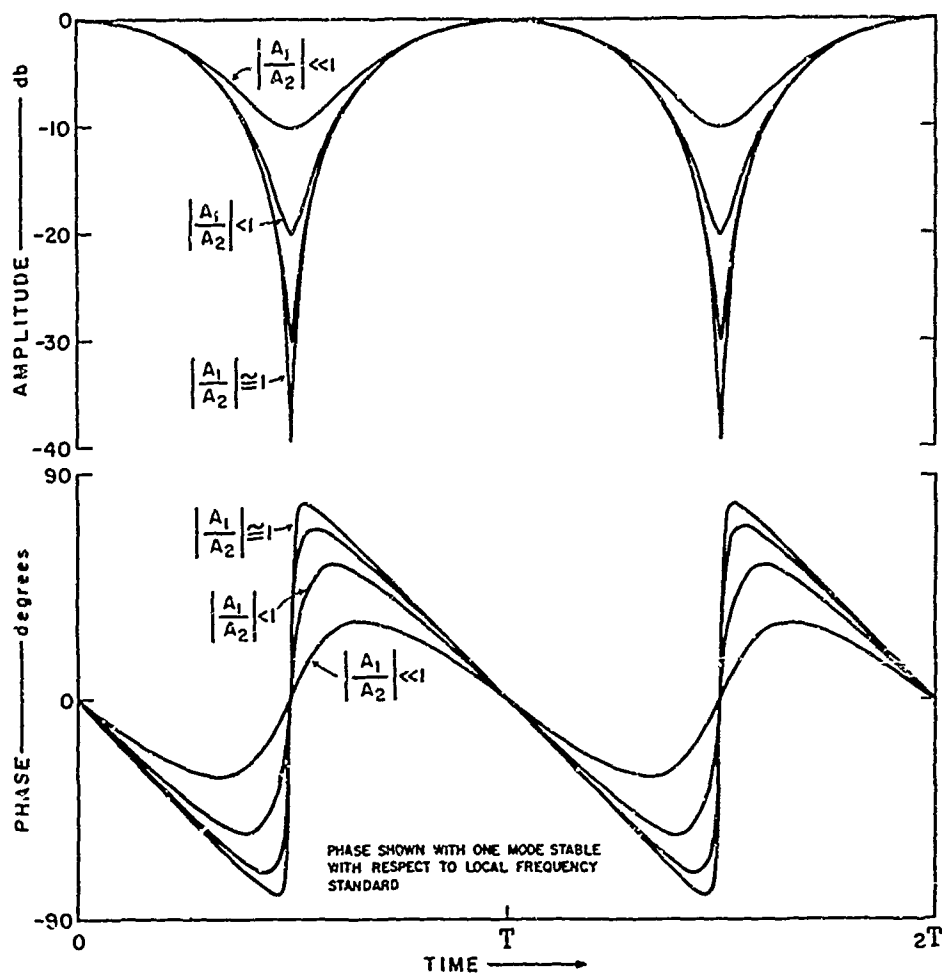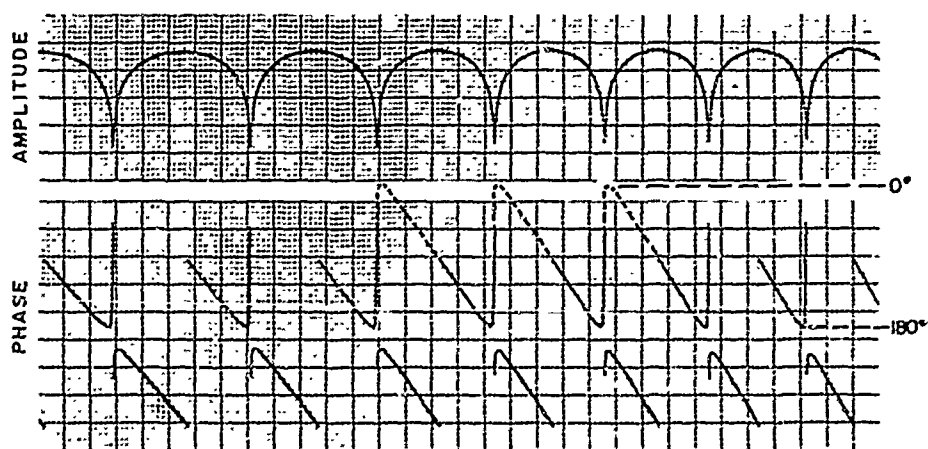
68

FIG. 34(a) THEORETICAL AMPLITUDE AND PHASE OF A TWO-MODE
CW SIGNAL

FIG. 34(b) SAMPLE WAVEFORMS — STABLE FREQUENCY AND AMPLITUDE
TEST (5102)

59

for comparison. During analysis, it was determined that the off-frequency signal contained 48.8 percent of the total power and the on-frequency signal 51.2 percent. The operation of the phase detector causes a signal with constant offset frequency to be displayed as a sawtooth waveform, discontinuous at multiples of 180^0. Adjusting for this 180^0 phase shift by dotted lines, the synthesized plots and the theoretical plots are identical.

Felperin[9] computed the amplitude density for two modes with some scatter as shown in Fig. 35. Figure 36, which shows the actual amplitude density as computed from the data, closely resembles the theoretical density plot. The jagged appearance of the experimental plot is probably caused by insufficient sampling. As in the computed case, two main peaks appear, corresponding to the sum and difference of the two input signal amplitudes. The difference between the two amplitudes (shown by the first peak) is somewhat less in the experimental case than in the computed case, although the sum, shown by the second and main peak, is approximately the same.

The power spectrum shown in Fig. 37 shows only the off-frequency mode approximately 0.05 cps above 7.366 Mc. The on-frequency signal, which was the output of the frequency synthesizer operating in its frequency-locked mode of operation, is not shown, as was discussed in Sec. III-1. Since no trace of this signal can be seen on the spectrum, it must be concluded that it was extremely stable and did not deviate from center frequency. The off-frequency signal was the output of the calibration oscillator. Its frequency deviation is even smaller than that of the frequency synthesizer in unlocked operation, as that frequency synthesizer was used in the previous test. For this off-frequency spike, the equivalent-triangle base width is only 0.125 cps as compared with a best possible figure of 0.111 cps. Therefore it appears that the frequency spreading of the previous test (where the base width was 0.155 cps) was caused either by the unlocked frequency synthesizer or by some transient effect, because the system is otherwise unchanged.
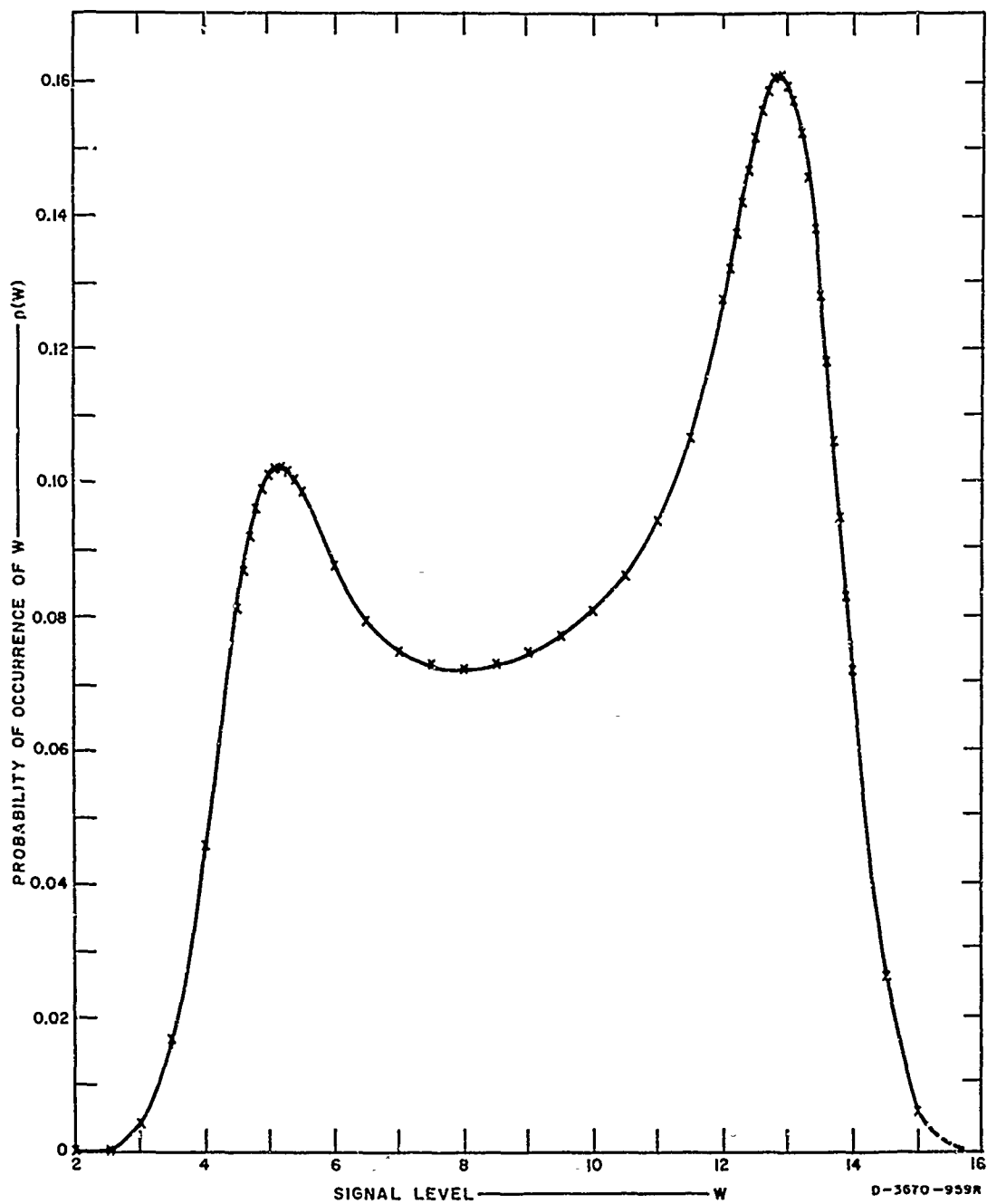
60

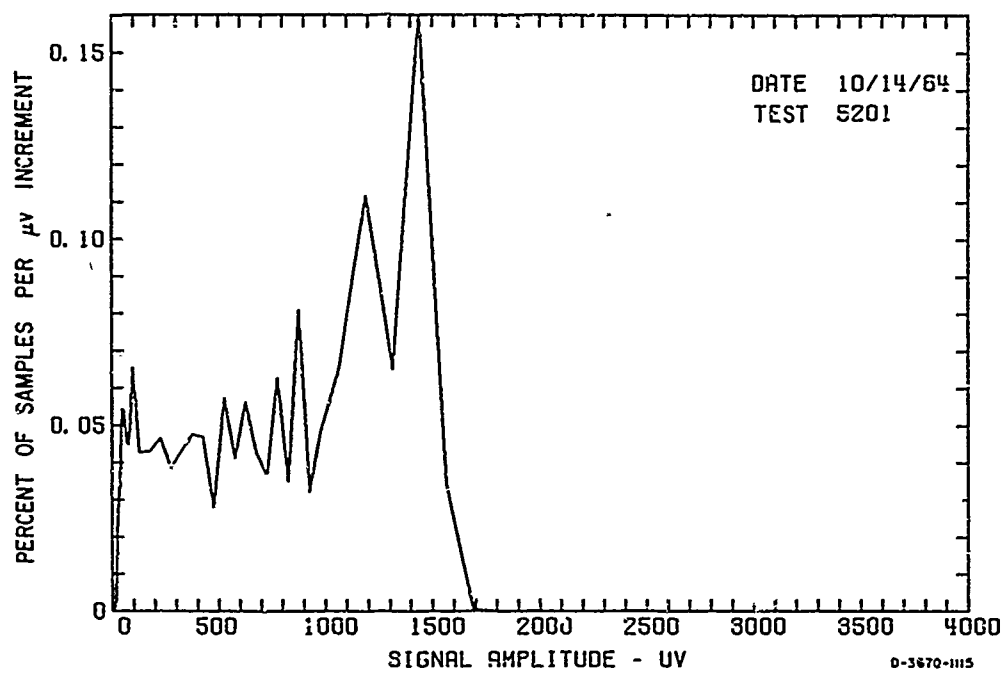FIG. 35 AMPLITUDE DENSITY-THEORETICAL TWO-MODE GENERAL CASE — SMALL SCATTER

61

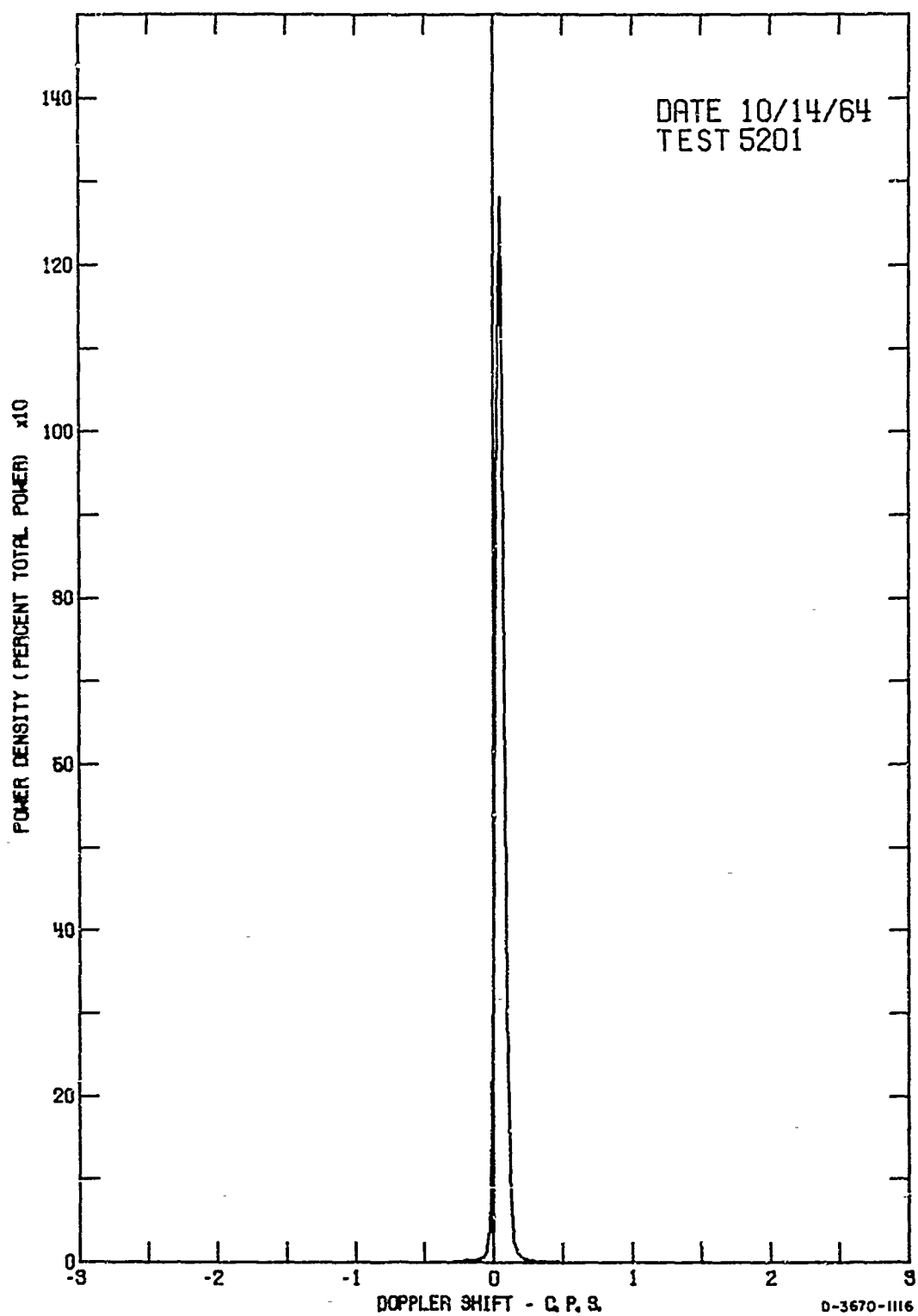FIG. 36 AMPLITUDE DENSITY (μv) — TWO-MODE TEST (5201)

62

FIG. 37 POWER SPECTRUM TWO-MODE TEST (5201)

63

The phase change plot for the two-mode test (5201), Fig. 38, shows that the slow phase drift between nulls in the fading pattern appears on the positive side. The rapid negative phase shift at the null of the fade is apparent on the plot as a high occurrence of large negative phase shift.

B. Frequency Accuracy of the Phase-Stable System

To minimize the frequency difference between site standards, a phase comparator was designed for comparison of the frequency of a local frequency standard with a VLF standard-frequency transmission. A VLF reference was used because of the relatively constant phase and long-range characteristics of VLF propagation. The phase difference between a submultiple of the local frequency standard and the reference VLF transmission was recorded on a 7-day circular chart by the phase comparator. From this chart, shown in Fig. 39, the rate of frequency drift can be calculated and the standard correction can be determined. In practice, the frequency of the standard was over-corrected each day by one-half the daily frequency drift. This procedure allowed the standard to drift through zero frequency error between corrections.[1]

A frequency difference between the transmitter and receiver site frequency standards will shift the Doppler frequency spikes on the power spectrum plot. A frequency difference of less than 1/40 cps will not cause apparent Doppler offset as the power spectrum estimates are made every 1/40 cps.[8] However, if the difference between site frequency standards approaches the 1/40-cps resolution value, spikes on the power spectrum will be shifted by the frequency difference between standards. This effect is shown in Fig. 40.

Frequency difference between the standards of both transmitter sites and the receiver site near Palo Alto was calculated from correction data for February and June,1964, to determine if any error due to frequency offset occurred on system plots. Maximum daily frequency difference is plotted in Fig. 41. If the frequency of the standard at the transmitting site was higher than that of the receiver site standard, the signal would have an apparent positive Doppler shift. The magnitude

64
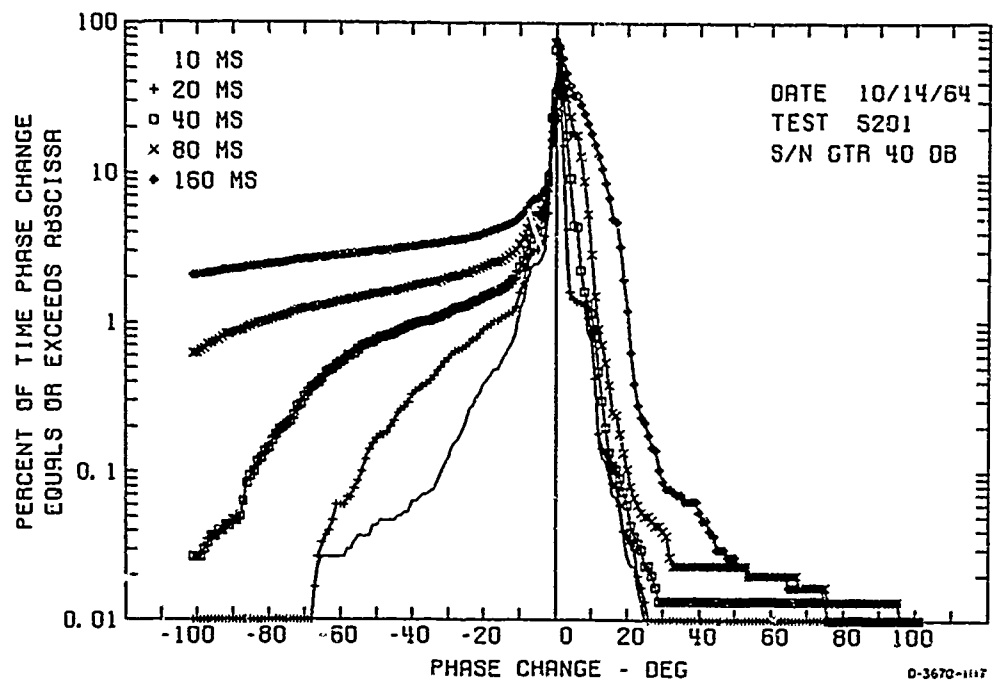
FIG. 38 PHASE DISTRIBUTION (S/N > 40 db) — TWO-MODE TEST (5201)
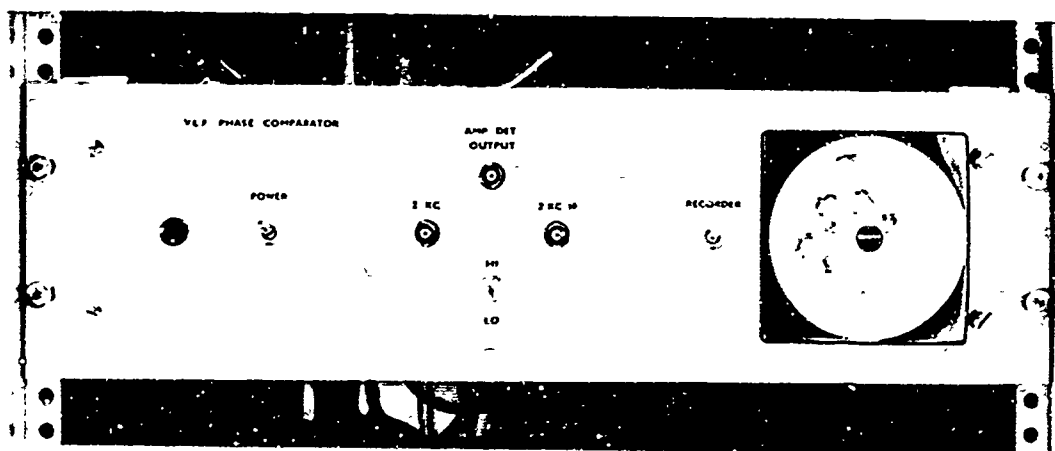
FIG. 39 VLF PHASE COMPARATOR

65
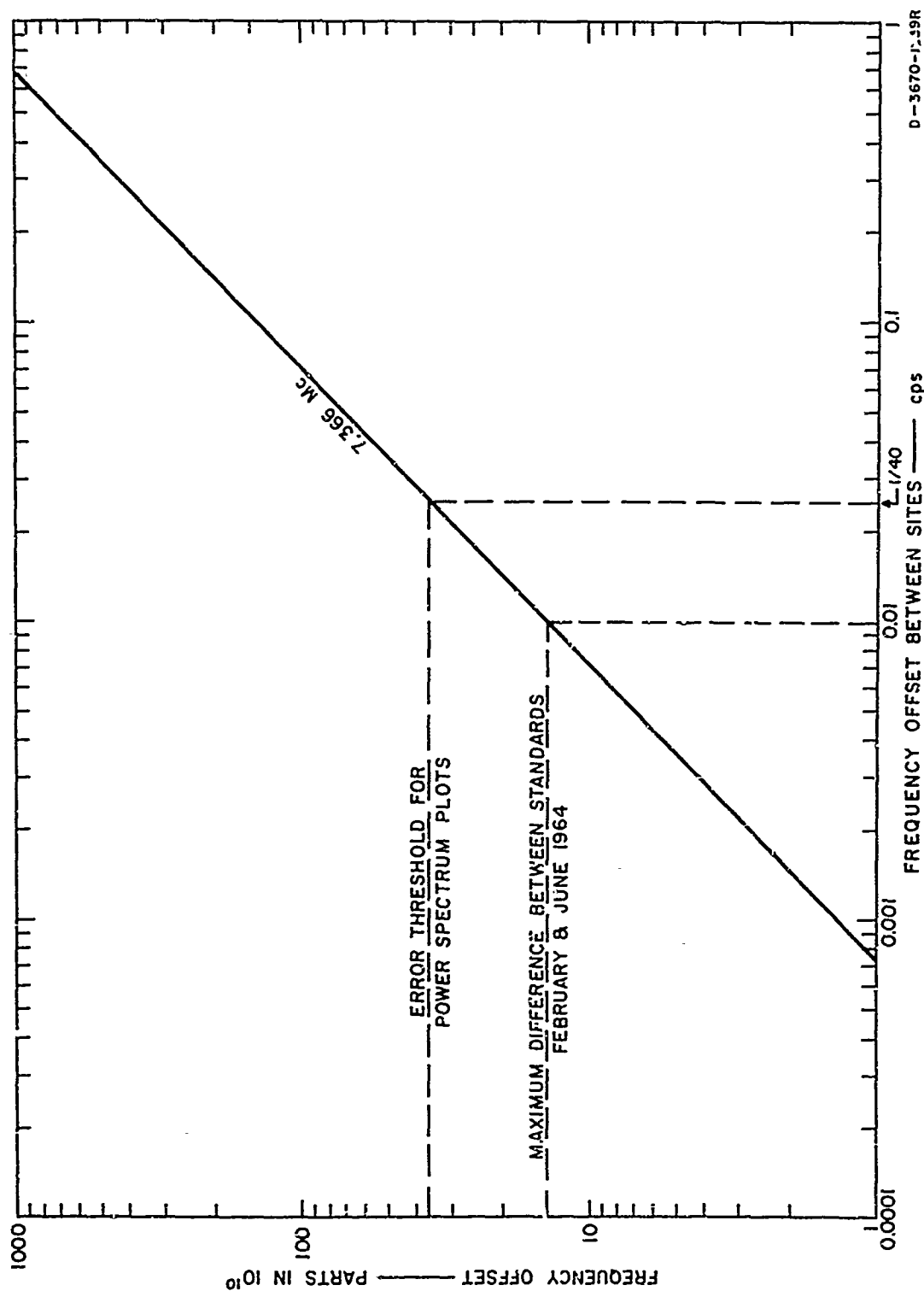
FIG. 40 RELATIONSHIP OF FREQUENCY STANDARD OFFSET TO POWER SPECTRUM ERROR
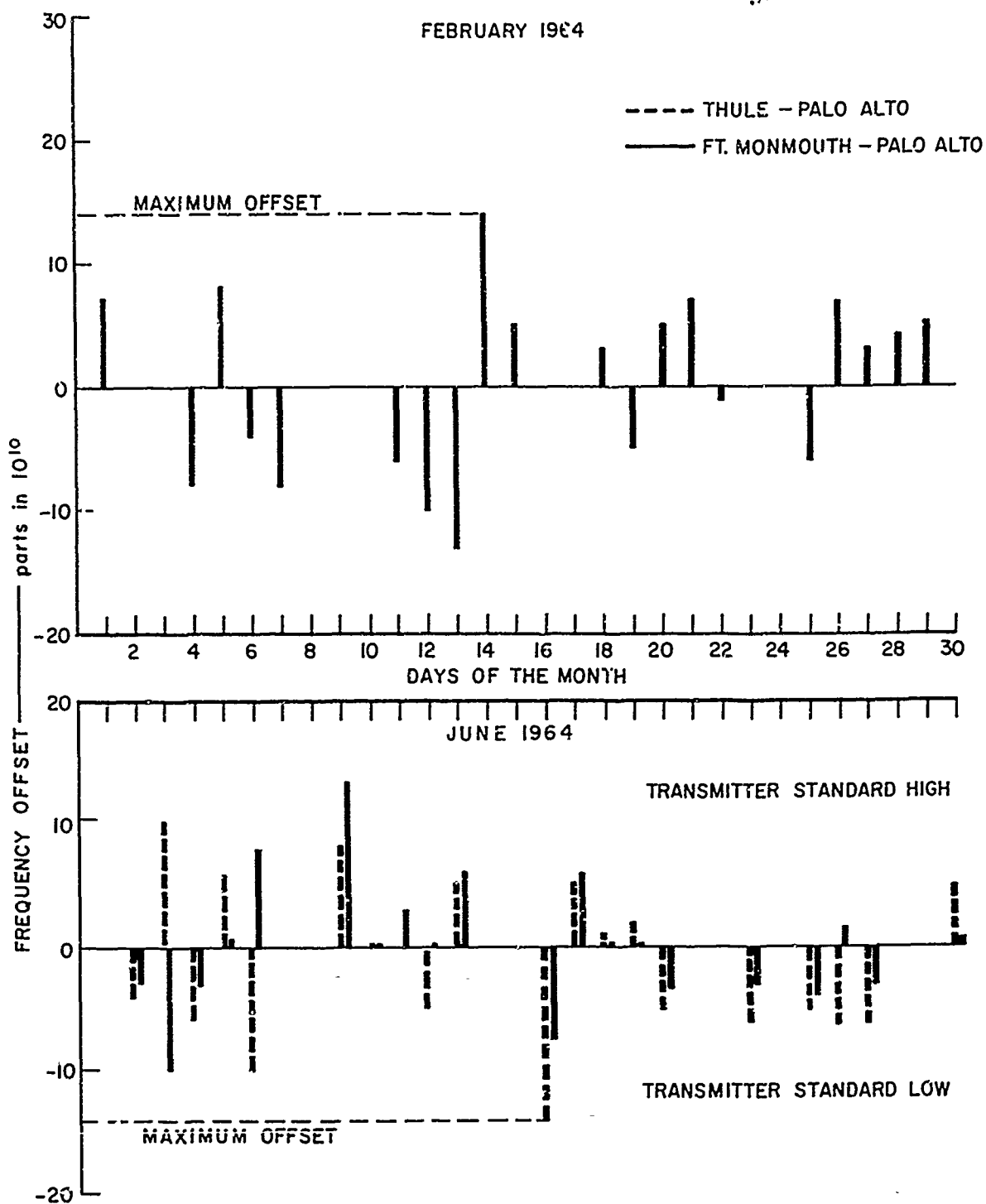
FIG. 41 MAXIMUM DAILY FREQUENCY OFFSET BETWEEN SITES — FEBRUARY
AND JUNE 1964

of the 1/40-cps error threshold is indicated on Fig. 40 as ± 36 parts in 10^{10}. During the two months plotted, all sites except Thule used the WWVL VLF transmission as a reference for correction; Thule used GBR, Great Britain. The average daily error of GBR with respect to WWVL was +2.03 and +2.15 parts in 10^{11} for February and June, respectively.

The maximum frequency difference between site frequency standards for these months was -14 parts in 10^{10}, the average difference being much smaller. From Fig. 40, this maximum difference contributed a system error of -0.01 cps, which is well within the 1/40-cps tolerance of the power spectrum plot. Consequently, the magnitude of the maximum daily frequency difference found during the two months studied did not cause Doppler frequency offset.

REFERENCES

1. R. A. Shepherd, "HF Communication Effects Simulation: Instrumentation and Operation of the Field Experiment," Interim Report 3, Contract DA 36-039 SC-87197, DASA Subtask 938/04-014, SRI Project 3670, Stanford Research Institute, Menlo Park, California (December 1963). AD-434 554.

2. R. F. Daly, "On Modeling the Time-Varying Frequency-Selective Radio Channel," Tech. Report 2--Part II, Contract DA 36-039 SC-90859, SRI Project 4172, Stanford Research Institute, Menlo Park, California (July 1964).

3. R. F. Daly, "Analysis of Multipath Effects on FSK Error Probability for a Simple HF Channel Model," Research Memorandum 1, Contract SD-189, SRI Project 4554, Stanford Research Institute, Menlo Park, California (February 1964).

4. N. T. Gaarder, "An Error-Rate Expression for HF DPSK Communications Systems," Tech. Report 3, Contract DA 36-039 SC-90859, SRI Project 4172, Stanford Research Institute, Menlo Park, California (August 1964).

5. J. W. Koch, W. M. Beery, and H. E. Petrie, "Experimental Studies of Fading and Phase Characteristics of High-Frequency Signals Propagated Through Auroral Regions," NBS Report 6701, NBS Project 8540-12-85441, National Bureau of Standards, Boulder, Colorado (June 3, 1960).

6. D. G. Brennan and M. Lindeman Phillips, "Phase and Amplitude Variability in Medium-Frequency Ionospheric Transmission," Tech. Report 93, Massachusetts Institute of Technology, Lincoln Laboratory, Lexington, Massachusetts (16 September 1957).

7. "Study of Fine Grain Fading and Phase Stability of Multiple CW Signals," Report 3 for Task 3, Interim Technical Report for Period 1 January 1962 to 31 August 1962, Contract DA 36-039 SC 88943, Department of the Army Project 3B-24-01-003-14, General Dynamics/Electronics-Rochester, Rochester, New York (No date).

8. R. F. Daly, "A Power Spectrum Program for Estimating the Doppler Profile of a Radio Channel," Research Memorandum 15, Contract DA 36-039 SC-87197, NWER Subtask 04.104, SRI Project 3670, Stanford Research Institute, Menlo Park, California (October 1964) DASA 1531.

9. K. D. Felperin, "Amplitude Distribution Due to Multipath and Scatter: A Theoretical Model," Research Memorandum 12, Contract DA 36-039 SC-87197, DASA Subtask 938/04-014, SRI Project 3670, Stanford Research Institute, Menlo Park, California (January 1964).

DOCUMENT CONTROL DATA - R&D

(Security classification of title, body of abstract and indexing annotation must be entered when the overall report is classified)

1. ORIGINATING ACTIVITY (Corporate author)	2a. REPORT SECURITY CLASSIFICATION
Stanford Research Institute	Unclassified
Menlo Park, California	2b GROUP N/A

3. REPORT TITLE

HF COMMUNICATION EFFECTS:
PHASE-STABLE DATA REDUCTION TECHNIQUES AND SYSTEM TEST RESULTS

4. DESCRIPTIVE NOTES *(Type of report and inclusive dates)*

Final Report

5. AUTHOR(S) *(Last name, first name, initial)*

Shepherd, R. A. - Tupper, B. C. - Lomax, J. B.

6. REPORT DATE	7a. TOTAL NO. OF PAGES	7b. NO. OF REFS
August 1965	69	9

8a. CONTRACT OR GRANT NO.	9a. ORIGINATOR'S REPORT NUMBER(S)
DA 36-039 SC-87197	
b. PROJECT NO.	None
DASA NWER Subtask 938/07.041	
c.	9b. OTHER REPORT NO(S) (Any other numbers that may be assigned this report)
d. SRI Project 3670	DASA #1691

10. AVAILABILITY/LIMITATION NOTICES

Qualified requesters may obtain copies of this report from L/C.
This report has not been processed or approved for open publication.

11. SUPPLEMENTARY NOTES	12. SPONSORING MILITARY ACTIVITY
	U.S. Army Electronics Command (AMSEL-NL-R-4) Fort Monmouth, New Jersey

13. ABSTRACT

Data-reduction techniques are discussed for the phase-stable CW system developed by Stanford Research Institute under contract from the U.S. Army Electronics Command and the Defense Atomic Support Agency.

An experiment was conducted in which signals were received at a site near Palo Alto over a transauroral path from Thule, Greenland and over a mid-latitude path from Fort Monmouth, New Jersey.

Fixed-frequency, 7.366-Mc phase-stable data collected in analog form on magnetic tape during the field portion of the experiment were digitized and reduced on an IBM 7090 computer to plot form. Examples of distributions of amplitude, rate of change of amplitude, and rate of change of phase are presented. Power spectra of the received signal are shown.

Several special tests were conducted to determine the resolution of the equipment and the results of these tests are discussed. Equipment limitations that must be considered in interpreting the data from the phase-stable system are pointed out.

DD FORM 1473
1 JAN 64

14. KEY WORDS	LINK A		LINK B		LINK C	
	ROLE	WT	ROLE	WT	ROLE	WT
Radio Communication Systems						
Ionospheric Propagation						
HF Radio Communication						
Mid-Latitude Path Propagation Measurements						
Arctic Path Propagation Measurements						
Amplitude Change Distributions						
Phase Change Distributions						

INSTRUCTIONS

1. **ORIGINATING ACTIVITY:** Enter the name and address of the contractor, subcontractor, grantee, Department of Defense activity or other organization *(corporate author)* issuing the report.

2a. **REPORT SECURITY CLASSIFICATION:** Enter the overall security classification of the report. Indicate whether "Restricted Data" is included. Marking is to be in accordance with appropriate security regulations.

2b. **GROUP:** Automatic downgrading is specified in DoD Directive 5200.10 and Armed Forces Industrial Manual. Enter the group number. Also, when applicable, show that optional markings have been used for Group 3 and Group 4 as authorized.

3. **REPORT TITLE:** Enter the complete report title in all capital letters. Titles in all cases should be unclassified. If a meaningful title cannot be selected without classification, show title classification in all capitals in parenthesis immediately following the title.

4. **DESCRIPTIVE NOTES:** If appropriate, enter the type of report, e.g., interim, progress, summary, annual, or final. Give the inclusive dates when a specific reporting period is covered.

5. **AUTHOR(S):** Enter the name(s) of author(s) as shown on or in the report. Enter last name, first name, middle initial. If military, show rank and branch of service. The name of the principal author is an absolute minimum requirement.

6. **REPORT DATE:** Enter the date of the report as day, month, year; or month, year. If more than one date appears on the report, use date of publication.

7a. **TOTAL NUMBER OF PAGES:** The total page count should follow normal pagination procedures, i.e., enter the number of pages containing information.

7b. **NUMBER OF REFERENCES:** Enter the total number of references cited in the report.

8a. **CONTRACT OR GRANT NUMBER:** If appropriate, enter the applicable number of the contract or grant under which the report was written.

8b, 8c, & 8d. **PROJECT NUMBER:** Enter the appropriate military department identification, such as project number, subproject number, system numbers, task number, etc.

9a. **ORIGINATOR'S REPORT NUMBER(S):** Enter the official report number by which the document will be identified and controlled by the originating activity. This number must be unique to this report.

9b. **OTHER REPORT NUMBER(S):** If the report has been assigned any other report numbers *(either by the originator or by the sponsor)*, also enter this number(s).

10. **AVAILABILITY/LIMITATION NOTICES:** Enter any limitations on further dissemination of the report, other than those imposed by security classification, using standard statements such as:

  (1) "Qualified requesters may obtain copies of this report from DDC."

  (2) "Foreign announcement and dissemination of this report by DDC is not authorized."

  (3) "U. S. Government agencies may obtain copies of this report directly from DDC. Other qualified DDC users shall request through
_____."

  (4) "U. S. military agencies may obtain copies of this report directly from DDC. Other qualified users shall request through
_____."

  (5) "All distribution of this report is controlled. Qualified DDC users shall request through
_____."

If the report has been furnished to the Office of Technical Services, Department of Commerce, for sale to the public, indicate this fact and enter the price, if known.

11. **SUPPLEMENTARY NOTES:** Use for additional explanatory notes.

12. **SPONSORING MILITARY ACTIVITY:** Enter the name of the departmental project office or laboratory sponsoring *(paying for)* the research and development. Include address.

13. **ABSTRACT:** Enter an abstract giving a brief and factual summary of the document indicative of the report, even though it may also appear elsewhere in the body of the technical report. If additional space is required, a continuation sheet shall be attached.

It is highly desirable that the abstract of classified reports be unclassified. Each paragraph of the abstract shall end with an indication of the military security classification of the information in the paragraph, represented as *(TS), (S), (C), or (U).*

There is no limitation on the length of the abstract. However, the suggested length is from 150 to 225 words.

14. **KEY WORDS:** Key words are technically meaningful terms or short phrases that characterize a report and may be used as index entries for cataloging the report. Key words must be selected so that no security classification is required. Identifiers, such as equipment model designation, trade name, military project code name, geographic location, may be used as key words but will be followed by an indication of technical context. The assignment of links, rules, and weights is optional.

DD FORM 1473 (BACK)
1 JAN 64